arXiv:1607.01001v3 [hep-ph] 6 Oct 2016

Dark Matter from a Classically Scale-Invariant $\mathbf{SU(3)_X}$

Alexandros Karam[1*] **and Kyriakos Tamvakis**[1,2†]

[1] *University of Ioannina, Physics Department, Section of Theoretical Physics, GR–45110 Ioannina, Greece*

[2] *CERN, Theoretical Physics Department, Geneva 23, CH-1211, Switzerland*

Abstract

In this work we study a classically scale-invariant extension of the Standard Model in which the dark matter and electroweak scales are generated through the Coleman-Weinberg mechanism. The extra $SU(3)_X$ gauge factor gets completely broken by the vacuum expectation values of two scalar triplets. Out of the eight resulting massive vector bosons the three lightest are stable due to an intrinsic $Z_2 \times Z_2'$ discrete symmetry and can constitute dark matter candidates. We analyze the phenomenological viability of the predicted multi-Higgs sector imposing theoretical and experimental constraints. We perform a comprehensive analysis of the dark matter predictions of the model solving numerically the set of coupled Boltzmann equations involving all relevant dark matter processes and explore the direct detection prospects of the dark matter candidates.

KEYWORDS: Classical Scale Invariance, Beyond Standard Model, Higgs boson, Dark Matter

*email: alkaram@cc.uoi.gr
†email: tamvakis@uoi.gr

Contents

1 Introduction **2**

2 The Model **4**
- 2.1 Tree-level potential . . . 4
- 2.2 Scalar masses . . . 6
- 2.3 Dark gauge boson masses . . . 7
- 2.4 One-loop potential . . . 9

3 Phenomenological analysis **10**

4 Dark matter analysis **13**
- 4.1 Boltzmann equations and relic density . . . 15
  - 4.1.1 Case $v_1^2 \gg v_2^2$ . . . 19
  - 4.1.2 Case $v_1 \simeq v_2$ . . . 20
- 4.2 Direct detection . . . 23

5 Summary and conclusions **24**

A Oblique Parameters **25**

B RGEs **26**

C Kinematics **27**

---

1. Introduction

The first run of the LHC culminated with the discovery [1, 2] of the 125 GeV Higgs boson [3–6]. The Standard Model (SM) is now complete and has successfully passed every experimental test. Nevertheless, it comes short of describing various phenomena such as the nature of dark matter, the nonzero neutrino masses, the asymmetry between matter and antimatter. It also cannot explain the origin of the electroweak scale and why strong interactions seem to preserve the CP symmetry. A more fundamental theory should be able to address these issues and also accommodate a particle physics description of cosmological inflation. The second run of the LHC is now underway and

will hopefully provide us with solutions to some of these problems and point us to a direction for physics beyond the Standard Model.

In the SM, the Higgs field H enters the Lagrangian through the scalar potential

$$V(H) = -m^2 H^\dagger H + \lambda_h \left(H^\dagger H\right)^2 , \tag{1.1}$$

where λ_h is the Higgs self-coupling and $m^2 > 0$ is the mass parameter responsible for spontaneously breaking the electroweak symmetry. The latter is the only dimensionful parameter in the SM and its quadratic sensitivity with respect to higher scales is what causes the *hierarchy problem*. Setting $m^2 = 0$ results in a manifestly classically scale-invariant (CSI) theory [7]. In 1973 Coleman and E. Weinberg (CW) [8] considered scalar QED and showed that classical scale symmetry gets broken at the quantum level due to logarithmic corrections and that the gauge symmetry breaking scale can arise through *dimensional transmutation*. Three years later Gildener and S. Weinberg (GW) [9] generalized their mechanism by considering an arbitrary number of scalar fields. However, an implementation of the CW mechanism in the SM is not phenomenologically viable due to the large top mass that renders the effective potential unstable. This situation can be remedied by extending the SM with new scalar and/or vector degrees of freedom which contribute positively to the effective potential.

The measured value of the Higgs boson mass $M_h = 125.09 \pm 0.24$ GeV [10] gives $\lambda(M_t) \approx 0.1285$ [11,12] at the scale of the top mass. Because of the large contribution of the top Yukawa coupling in its renormalization group equation (RGE), λ_h runs negative above scales of $\mathcal{O}(10^{10}\,\text{GeV})$ which results in the vacuum being in a metastable state [13–22]. In order to (fully) stabilize the potential, one needs to couple the Higgs field with extra bosonic fields that contribute positively to the RGE of λ_h.

A classically scale invariant extension of the SM can in principle solve both the hierarchy and the vacuum stability problems. Various CSI models have recently been proposed. The authors of [23–61] extended only the scalar sector, while the authors of [62–102] extended the gauge sector as well with Abelian or non-Abelian gauge symmetries. Some of these models have the appealing feature that they also predict stable and weakly interacting massive particles (WIMPs) which can be viable candidates for dark matter (DM).

In this work, we propose a CSI extension of the SM where a new $SU(3)_X$ gauge symmetry can provide massive gauge fields that can account for the observed DM relic density. The hidden sector will be broken completely by two scalar triplets. These will have portal couplings with the Higgs field and will help in the stabilization of the potential. The scalar sector will consist of three Higgs-like particles, one of which will be massless at tree level but will nevertheless acquire a nonzero mass once we consider the full one-loop scalar potential. All eight of the extra gauge bosons will become massive, while the three lightest will be stable due to their parities under an intrinsic $Z_2 \times Z_2'$ discrete symmetry of $SU(3)_X$. These three dark gauge bosons will be our DM candidates. Because of the rich structure of the extra gauge group, the computation of the DM relic density will include various types of processes apart from DM annihilations, such as semiannihilations, coannihilations, and DM conversions.

The layout of the paper is the following. In the next section we present the model and calculate the masses of the new fields. In Sec. 3 we impose various theoretical and experimental constraints on the model. Then, in Sec. 4 we give a detailed analysis of the system of Boltzmann equations that need to be solved in order to obtain the DM relic abundance, and we also focus on the role of coannihilations and DM conversion processes. Furthermore, we examine the direct detection prospects of the DM candidates. Finally, we summarize and conclude in Sec. 5. Useful formulas are presented in Appendices A, B, and C.

2. The Model

We begin with a CSI version of the Standard Model and consider an $SU(3)_X$ extension of its gauge symmetry in order to accommodate the presence of dark matter. The non-CSI version of this model was recently considered in Ref. [103]. The breaking of the gauge symmetry $SU(3)_C \times SU(2)_L \times U(1)_Y \times SU(3)_X \to SU(3)_C \times U(1)_{em}$ is achieved through the Coleman-Weinberg mechanism [8]. In addition to the new $SU(3)_X$ gauge bosons, referred to as "dark" gauge bosons, the model contains a pair of complex scalars $\Phi_1(1,1,0;3)$ and $\Phi_2(1,1,0;3)$ transforming as singlets under the Standard Model gauge group and as triplets under $SU(3)_X$, referred to as "dark" scalars. In this section we explore the scalar and gauge sectors of the model. First, we present the tree-level potential. Employing the Gildener-Weinberg formalism [9], we minimize the tree-level potential at a definite energy scale which defines a flat direction among the scalar fields. Then, we compute the tree-level scalar and dark gauge boson masses. One of the scalar bosons turns out to be massless at tree level and corresponds to the pseudo–Nambu-Goldstone boson (pNGB) of broken scale symmetry. Finally, we present the one-loop effective potential which becomes dominant along the flat direction and greatly lifts the mass of the pNGB.

2.1. Tree-level potential

The most general renormalizable and scale-invariant tree-level scalar potential involving the standard Higgs doublet H and the dark triplets Φ_1, Φ_2 is

$$\begin{aligned} V_0 \;=\; & \lambda_h (H^\dagger H)^2 \;+\; \lambda_1 (\Phi_1^\dagger \Phi_1)^2 + \lambda_2 (\Phi_2^\dagger \Phi_2)^2 - \lambda_3 (\Phi_1^\dagger \Phi_1)(\Phi_2^\dagger \Phi_2) + \lambda_4 (\Phi_1^\dagger \Phi_2)(\Phi_2^\dagger \Phi_1) \\ & + \left[\frac{\lambda_5}{2} (\Phi_1^\dagger \Phi_2)^2 + \lambda_6 (\Phi_1^\dagger \Phi_1)(\Phi_1^\dagger \Phi_2) + \lambda_7 (\Phi_2^\dagger \Phi_2)(\Phi_1^\dagger \Phi_2) + \text{H.c.} \right] - \lambda_{h1} (H^\dagger H)(\Phi_1^\dagger \Phi_1) \\ & + \;\lambda_{h2} (H^\dagger H)(\Phi_2^\dagger \Phi_2) \;- \Big(\lambda_{h12} (H^\dagger H)(\Phi_1^\dagger \Phi_2) + \text{H.c.} \Big) \,, \end{aligned} \tag{2.1}$$

where all appearing coupling constants are taken to be real and positive. Notice that we have assumed negative signs for the λ_{h1} and λ_3 portal couplings as the basic seed of symmetry breaking. Out of the 12 degrees of freedom included in Φ_1, Φ_2, 8 are Higgsed away. Using gauge freedom and

removing 5 of them from Φ_1 and 3 from Φ_2, we end up in the unitary gauge with Φ_1 containing 1 and Φ_2 3 real degrees of freedom

$$\Phi_1 \;=\; \frac{1}{\sqrt{2}}\begin{pmatrix} 0 \\ \\ 0 \\ \\ v_1+\phi_1 \end{pmatrix}, \qquad \Phi_2 \;=\; \frac{1}{\sqrt{2}}\begin{pmatrix} 0 \\ \\ v_2+\phi_2 \\ \\ (v_3+\phi_3)+i(v_4+\phi_4) \end{pmatrix}. \tag{2.2}$$

Assuming CP invariance implies that all vacuum expectation values (VEVs) are real and $v_4 = 0$. The extra $SU(3)_X$ can be completely broken if at least two of the remaining VEVs are nonzero, so we further assume $v_3 = 0$ for simplicity. The standard Higgs will correspond to 1 real degree of freedom

$$H \;=\; \frac{1}{\sqrt{2}}\begin{pmatrix} 0 \\ \\ v_h+h \end{pmatrix}. \tag{2.3}$$

The scalar potential is further simplified if we impose invariance of the potential under the discrete symmetry

$$\Phi_2 \to\; -\Phi_2, \tag{2.4}$$

which implies

$$\lambda_6 = \lambda_7 = \lambda_{h12} = 0. \tag{2.5}$$

Omitting the VEVs for the moment, the resulting potential is

$$\begin{aligned} V_0 \;=\; & \frac{\lambda_h}{4}h^4 + \frac{\lambda_1}{4}\phi_1^4 + \frac{\lambda_2}{4}\phi_2^4 - \frac{\lambda_{h1}}{4}h^2\phi_1^2 + \frac{\lambda_{h2}}{4}h^2\phi_2^2 - \frac{\lambda_3}{4}\phi_1^2\phi_2^2 \\ & + \frac{\lambda_2}{4}(\phi_3^2+\phi_4^2)^2 + \left(\frac{\lambda_2}{2}\phi_2^2 + \frac{\lambda_3}{4}\phi_1^2 + \frac{\lambda_4}{4}\phi_1^2 + \frac{\lambda_{h2}}{4}h^2\right)\left(\phi_3^2+\phi_4^2\right) + \frac{\lambda_5}{4}\phi_1^2\left(\phi_3^2-\phi_4^2\right). \end{aligned} \tag{2.6}$$

The above potential is bounded from below if the following conditions [104–106] are satisfied for all energies up to the Planck scale[1]:

$$\lambda_h \;\geq\; 0,\; \lambda_1 \;\geq\; 0,\; \lambda_2 \;\geq\; 0, \tag{2.7}$$

$$2\sqrt{\lambda_h\lambda_1} - \lambda_{h1} \geq 0, \quad 2\sqrt{\lambda_h\lambda_2} + \lambda_{h2} \geq 0, \quad 2\sqrt{\lambda_1\lambda_2} - \lambda_3 \geq 0, \tag{2.8}$$

$$4\lambda_h\lambda_1\lambda_2 - \left(\lambda_{h1}^2\lambda_2 + \lambda_{h2}^2\lambda_1 + \lambda_3^2\lambda_h\right) + \lambda_{h1}\lambda_{h2}\lambda_3 \;\geq\; 0. \tag{2.9}$$

[1] In fact, a more rigorous treatment shows that we must replace λ_3 with $\lambda_3 + \min\left[0, \lambda_4+\lambda_5, \lambda_4-\lambda_5\right]$ in the stability conditions (2.7)–(2.9). However, we shall assume $\lambda_4+\lambda_5 > 0$ and $\lambda_4-\lambda_5 > 0$, resulting in positive masses for the fields ϕ_3 and ϕ_4 [cf. (2.24)–(2.25)]. Therefore $\min\left[0, \lambda_4+\lambda_5, \lambda_4-\lambda_5\right] = 0$.

2.2. Scalar masses

Gauge symmetry breaking to $SU(3)_C \times U(1)_{em}$ can arise through the nonzero VEVs v_h, v_1, v_2. Since the tree-level potential does not contain any dimensionful parameters, this can only occur via the Coleman-Weinberg mechanism [8]. Having multiple scalars, we will make use of the Gildener-Weinberg approach [9] in order to minimize the potential. The tree-level potential is minimized at a particular renormalization scale $\mu = \Lambda$ which defines the flat direction among the VEVs. The corresponding equations read [9]

$$\lambda_h(\Lambda)\, v_h^4 + \lambda_1(\Lambda)\, v_1^4 + \lambda_2(\Lambda)\, v_2^4 - \lambda_3(\Lambda)\, v_1^2 v_2^2 - \lambda_{h1}(\Lambda)\, v_h^2 v_1^2 + \lambda_{h2}(\Lambda)\, v_h^2 v_2^2 = 0, \quad (2.10)$$

$$2\lambda_h(\Lambda)\, v_h^2 - \lambda_{h1}(\Lambda)\, v_1^2 + \lambda_{h2}(\Lambda)\, v_2^2 = 0, \quad (2.11)$$

$$2\lambda_1(\Lambda)\, v_1^2 - \lambda_3(\Lambda)\, v_2^2 - \lambda_{h1}(\Lambda)\, v_h^2 = 0, \quad (2.12)$$

$$2\lambda_2(\Lambda)\, v_2^2 - \lambda_3(\Lambda)\, v_1^2 + \lambda_{h2}(\Lambda)\, v_h^2 = 0. \quad (2.13)$$

Along the flat direction, the shifted scalar fields may be written as

$$h = (\varphi + v)\, n_h, \quad \phi_1 = (\varphi + v)\, n_1, \quad \phi_2 = (\varphi + v)\, n_2, \quad (2.14)$$

where $\varphi^2 = h^2 + \phi_1^2 + \phi_2^2$ and the overall VEV v is $v^2 = v_h^2 + v_1^2 + v_2^2$, with $n_h^2 + n_1^2 + n_2^2 = 1$.

The mass matrix of the three scalar fields that participate in the symmetry breaking can be read off from the shifted tree-level potential to be

$$\mathcal{M}_0^2 = v^2 \begin{pmatrix} 2\lambda_h n_h^2 & -n_h n_1 \lambda_{h1} & n_h n_2 \lambda_{h2} \\ -n_h n_1 \lambda_{h1} & 2\lambda_1 n_1^2 & -n_1 n_2 \lambda_3 \\ n_h n_2 \lambda_{h2} & -n_1 n_2 \lambda_3 & 2\lambda_2 n_2^2 \end{pmatrix} \quad (2.15)$$

in the $(h,\, \phi_1,\, \phi_2)$ basis. Next, we may consider a general rotation

$$\mathcal{R}\, \mathcal{M}_0^2\, \mathcal{R}^{-1} = \mathcal{M}_d^2 \implies \begin{pmatrix} h \\ \phi_1 \\ \phi_2 \end{pmatrix} = \mathcal{R}^{-1} \begin{pmatrix} h_1 \\ h_2 \\ h_3 \end{pmatrix}, \quad (2.16)$$

in terms of the rotation matrix $\mathcal{R}^{-1}$ given by

$$\mathcal{R}^{-1} = \begin{pmatrix} \cos\alpha\cos\beta & \sin\alpha & \cos\alpha\sin\beta \\ -\cos\beta\cos\gamma\sin\alpha + \sin\beta\sin\gamma & \cos\alpha\cos\gamma & -\cos\gamma\sin\alpha\sin\beta - \cos\beta\sin\gamma \\ -\cos\gamma\sin\beta - \cos\beta\sin\alpha\sin\gamma & \cos\alpha\sin\gamma & \cos\beta\cos\gamma - \sin\alpha\sin\beta\sin\gamma \end{pmatrix}. \quad (2.17)$$

Two of these rotation angles may be chosen to be related to the flat direction through

$$\begin{aligned} n_h &= \sin\alpha, \\ n_1 &= \cos\alpha\cos\gamma, \\ n_2 &= \cos\alpha\sin\gamma. \end{aligned} \quad (2.18)$$

Then, $\mathcal{M}_d^2$ is diagonal, provided that the following relation is satisfied:

$$\tan 2\beta = \frac{v_h v_1 v_2 v \left(\lambda_{h2} + \lambda_{h1}\right)}{\left(\lambda_1 + \lambda_2 + \lambda_3\right) v_1^2 v_2^2 - \lambda_h v_h^2 v^2} \ . \tag{2.19}$$

The resulting tree-level masses include a zero eigenvalue, namely, $M_{h_2} = 0$, which corresponds to the pNGB of broken scale invariance. Of course, this mass will be strongly lifted at the one-loop level. The other two eigenvalues M_{h_1}, M_{h_3} are given by complicated expressions in terms of the overall VEV, the angles, and the scalar couplings. In addition to the above three scalar states there are also the scalar fields ϕ_3, ϕ_4, which we did not include in the above analysis. These fields do not receive a VEV but obtain tree-level masses as soon as the gauge symmetry breaking is established. As we will see in Sec. 2.4, radiative corrections will strongly affect only the flat direction defined by h_2, while the masses of ϕ_3, ϕ_4, h_1, h_3 will stay close to their tree-level values.

2.3. Dark gauge boson masses

The $SU(3)_X$ gauge fields enter the Lagrangian through the kinetic terms

$$\mathcal{L}_X = -\frac{1}{2}\,\mathrm{tr}\{X_{\mu\nu}X^{\mu\nu}\} + |D_\mu \Phi_1|^2 + |D_\mu \Phi_2|^2, \tag{2.20}$$

where the field strength tensor is defined as $X_{\mu\nu} = \partial_\mu X_\nu - \partial_\nu X_\mu + i g_X \left[X_\mu, X_\nu\right]$ and the covariant derivative of Φ_i has the form $D_\mu \Phi_i = \partial_\mu \Phi_i + i g_X X_\mu \Phi_i$.

Following Ref. [103], we consider the discrete symmetry $Z_2 \times Z_2'$ of the $SU(3)$ generators in the Gell-Mann basis, where the first Z_2 corresponds to a gauge transformation, while the second Z_2' is identified with complex conjugation. The parities of the gauge fields X_μ and the scalar fields Φ_i under $Z_2 \times Z_2'$ are summarized in Table 1. This discrete symmetry is important for the identification of dark matter since the lightest fields with nontrivial discrete signatures will not be able to decay to Standard Model matter.

Fields	$Z_2 \times Z_2'$
h, ϕ_1, ϕ_2, ϕ_3, X_μ^7	$(+,+)$
X_μ^2, X_μ^5	$(-,+)$
X_μ^1, X_μ^4	$(-,-)$
ϕ_4, X_μ^3, X_μ^6, X_μ^8	$(+,-)$

Table 1: Gauge and scalar fields parities under $Z_2 \times Z_2'$.

For the particular choice of nonzero $v_{1,2}$ and $v_{3,4} = 0$, there is only one mixing term, $X_\mu^3 X^{\mu 8}$, among the dark gauge fields. The gauge boson mass matrix has the form

$$\mathcal{M}_X^2 = \frac{g_X^2}{4}\begin{pmatrix} v_2^2 & 0 & 0 & 0 & 0 & 0 & 0 & 0 \\ 0 & v_2^2 & 0 & 0 & 0 & 0 & 0 & 0 \\ 0 & 0 & v_2^2 & 0 & 0 & 0 & 0 & -\frac{v_2^2}{\sqrt{3}} \\ 0 & 0 & 0 & v_1^2 & 0 & 0 & 0 & 0 \\ 0 & 0 & 0 & 0 & v_1^2 & 0 & 0 & 0 \\ 0 & 0 & 0 & 0 & 0 & v_1^2+v_2^2 & 0 & 0 \\ 0 & 0 & 0 & 0 & 0 & 0 & v_1^2+v_2^2 & 0 \\ 0 & 0 & -\frac{v_2^2}{\sqrt{3}} & 0 & 0 & 0 & 0 & \left(4v_1^2+v_2^2\right)/3 \end{pmatrix}. \tag{2.21}$$

Defining the gauge boson mass eigenstates as

$$\begin{pmatrix} X_\mu^{3'} \\ X_\mu^{8'} \end{pmatrix} = \begin{pmatrix} \cos\delta & \sin\delta \\ -\sin\delta & \cos\delta \end{pmatrix}\begin{pmatrix} X_\mu^3 \\ X_\mu^8 \end{pmatrix}, \tag{2.22}$$

with the mixing angle given by

$$\tan 2\delta = \frac{\sqrt{3}v_2^2}{2v_1^2 - v_2^2}, \implies \tan\delta = \frac{-2v_1^2 + v_2^2 \pm 2\sqrt{v_1^4 - v_1^2v_2^2 + v_2^4}}{\sqrt{3}v_2^2}, \tag{2.23}$$

we obtain the masses shown in Table 2. In the following, we keep only the " + " solution in (2.23) corresponding to $\tan\delta$ being small and positive for $v_1^2 \gg v_2^2$.

Gauge fields	Mass^2
X_μ^1	$\frac{1}{4}g_X^2v_2^2$
X_μ^2	$\frac{1}{4}g_X^2v_2^2$
$X_\mu^{3'}$	$\frac{1}{4}g_X^2v_2^2\left(1-\frac{\tan\delta}{\sqrt{3}}\right)$
X_μ^4	$\frac{1}{4}g_X^2v_1^2$
X_μ^5	$\frac{1}{4}g_X^2v_1^2$
X_μ^6	$\frac{1}{4}g_X^2\left(v_1^2+v_2^2\right)$
X_μ^7	$\frac{1}{4}g_X^2\left(v_1^2+v_2^2\right)$
$X_\mu^{8'}$	$\frac{1}{3}g_X^2v_1^2\left(1-\frac{\tan\delta}{\sqrt{3}}\right)^{-1}$

Table 2: Dark gauge boson masses.

In addition to the above gauge boson mass terms, the scalar kinetic terms also give a scalar/gauge-boson mixing

$$ig_X X_\mu^a(\partial^\mu\Phi_i)^\dagger T^a\Phi_i + H.c. \;=\; g_X\frac{v_2}{2}\left(\partial^\mu\phi_4\, X_\mu^6 - \partial^\mu\phi_3 X_\mu^7\right).$$

This leads to a redefinition of the two scalar and gauge fields involved according to

$$\tilde{X}^6_\mu = X^6_\mu + \tfrac{2}{g_X}\tfrac{v_2}{v_1^2+v_2^2}\partial_\mu\phi_4 \ , \quad \tilde{X}^7_\mu = X^7_\mu - \tfrac{2}{g_X}\tfrac{v_2}{v_1^2+v_2^2}\partial_\mu\phi_3,$$

$$\tilde{\phi}_3 = \tfrac{v_1}{\sqrt{v_1^2+v_2^2}}\phi_3 \ , \qquad \tilde{\phi}_4 = \tfrac{v_1}{\sqrt{v_1^2+v_2^2}}\phi_4.$$

The normalized masses for X_6, X_7 are the ones entering in Table 2, while the resulting masses of the canonical scalar fields $\tilde{\phi}_3$, $\tilde{\phi}_4$ are

$$M^2_{\tilde{\phi}_3} = \frac{1}{2}(\lambda_4+\lambda_5)\left(v_1^2+v_2^2\right) , \tag{2.24}$$

$$M^2_{\tilde{\phi}_4} = \frac{1}{2}(\lambda_4-\lambda_5)\left(v_1^2+v_2^2\right) . \tag{2.25}$$

For $v_1^2 \gg v_2^2$, the mixing angle δ is small and positive [cf. (2.23)], while $X^{1,2}_\mu$ and $X^{3'}_\mu$ are nearly degenerate in mass and also the lightest of the eight dark gauge bosons. In addition, because of their parities under $Z_2 \times Z_2'$ (cf. Table 1), they are stable and can therefore constitute DM candidates. Note, however, that $\tilde{\phi}_4$ and $X^{3'}_\mu$ have the same parities under $Z_2 \times Z_2'$. This means that the decay process $X^{3'} \to \tilde{\phi}_4 + \text{SM}$ is possible if $M_{\tilde{\phi}_4} < M_{X^{3'}}$, and in that case $\tilde{\phi}_4$ can be a DM candidate instead of $X^{3'}_\mu$. However, in the following we will study the case $M_{\tilde{\phi}_4} > M_{X^{3'}}$ and relegate this alternative scenario to future work.

2.4. One-loop potential

The one-loop potential, along the flat direction, at a renormalization scale $\mu = \Lambda$ where the tree-level potential is minimized, takes the form

$$V_1(\mathbf{n}\varphi) = A\,\varphi^4 + B\,\varphi^4\,\ln(\varphi^2/\Lambda^2)\,, \tag{2.26}$$

where the dimensionless coefficients A, B are given (in the $\overline{MS}$ scheme) by

$$A = \frac{1}{64\pi^2 v^4}\left[\sum_{i=h_1,h_3,\tilde{\phi}_3,\tilde{\phi}_4} M_i^4\left(-\frac{3}{2}+\log\frac{M_i^2}{v^2}\right) + 6M_W^4\left(-\frac{5}{6}+\log\frac{M_W^2}{v^2}\right) + 3M_Z^4\left(-\frac{5}{6}+\log\frac{M_Z^2}{v^2}\right)\right.$$
$$\left. +3\sum_{i=1}^{8} M_{X^i}^4\left(-\frac{5}{6}+\log\frac{M_{X^i}^2}{v^2}\right) - 12M_t^4\left(-1+\log\frac{M_t^2}{v^2}\right)\right], \tag{2.27}$$

$$B = \frac{1}{64\pi^2 v^4}\left(\sum_{i=h_1,h_3,\tilde{\phi}_3,\tilde{\phi}_4} M_i^4 + 6M_W^4 + 3M_Z^4 + 3\sum_{i=1}^{8} M_{X^i}^4 - 12M_t^4\right). \tag{2.28}$$

Note that the model, with its present minimal field content, does not accommodate neutrino mass generation through a right-handed neutrino seesaw mechanism. Nevertheless, right-handed neutrinos can still be present and obtain their mass from a separate sector, the minimal example being a real scalar field that couples only to neutrinos. Of course, with the given symmetries of the model, if such a singlet exists, its couplings with the rest of the scalars cannot be forbidden *a priori*. Nevertheless, it could be assumed that these couplings are quite small, in which case they would not affect the analysis of the rest of the model.

Minimizing the one-loop effective potential, we obtain

$$V_1(\mathbf{n}\varphi) \;=\; B\,\varphi^4\,\left[\ln\left(\frac{\varphi^2}{v^2}\right) - \frac{1}{2}\right]. \tag{2.29}$$

An immediate consequence of the one-loop radiative corrections is to lift the pNGB mass to the nonzero value

$$M_{h_2}^2 \;=\; \left.\frac{\partial^2 V_1}{\partial\varphi^2}\right|_{\varphi=v} \;=\; \frac{1}{8\pi^2 v^2}\left(M_{h_1}^4 + M_{h_3}^4 + M_{\tilde{\phi}_3}^4 + M_{\tilde{\phi}_4}^4 + 6M_W^4 + 3M_Z^4 + 3\sum_{i=1}^{8} M_{X^i}^4 - 12M_t^4\right). \tag{2.30}$$

Finally, note that the one-loop corrections to the masses of $\tilde{\phi}_{3,4}$ are exactly zero, while the corrections to the masses of $h_{1,3}$ are very suppressed and can be safely ignored to a first approximation.[2]

3. Phenomenological analysis

In this section we study the phenomenological viability of the model. First we examine the interrelationship among the masses of the dark gauge bosons and scalars. Then, scanning over a range of values for the scalar couplings and the dark gauge coupling we find benchmark points that satisfy stability and perturbativity constraints, as well as bounds set by the first run of the LHC and measurements of the electroweak precision observables.

The Coleman-Weinberg mechanism is successfully realized if the mass of the dark scalar M_{h_2} [cf. (2.30)] turns out to be positive. For this to be true we must have $B > 0$ [cf. (2.29)], or

$$M_{h_3}^4 + M_{\tilde{\phi}_3}^4 + M_{\tilde{\phi}_4}^4 + 3\sum_{i=1}^{8} M_{X_i}^4 > (317.26\ \text{GeV})^4\,. \tag{3.1}$$

The scalar state h_1 (that we identify with the Higgs boson) has analogous couplings to the SM particles as a SM Higgs, but rescaled by the factor $\mathcal{R}_{11}$ from the rotation matrix (2.17),

[2] See [33] for a complete treatment in a relevant CSI model.

$$g_{h_1\chi\chi} = \mathcal{R}_{11} g^{\rm SM}_{h\chi\chi}, \tag{3.2}$$

with $\chi\chi$ denoting a pair of SM particles. Constructing the signal strength parameter for h_1 [92],

$$\mu_{h_1} = \frac{\sigma\left(pp \to h_1\right)}{\sigma^{\rm SM}\left(pp \to h\right)} \frac{\mathrm{BR}\left(h_1 \to \chi\chi\right)}{\mathrm{BR}^{\rm SM}\left(h \to \chi\chi\right)} \simeq \cos^2\alpha \cos^2\beta, \tag{3.3}$$

and employing the bound set by the first run of the LHC [107–110]:

$$\mu_{h_1} > 0.81, \quad @\, 95\%\ \text{C.L.}, \tag{3.4}$$

we can constrain the matrix element $\mathcal{R}_{11}$ as

$$\mathcal{R}_{11} = \cos\alpha \cos\beta > 0.9\,, \tag{3.5}$$

meaning that the angles α, β cannot be too large.

Another experimental constraint arises from the measurements of the oblique parameters S, T, and U. Setting $U = 0$, we have [111]

$$S = 0.00 \pm 0.08, \qquad T = 0.05 \pm 0.07. \tag{3.6}$$

In this model, the above parameters are given by the formulas presented in Appendix A.

We can further constrain the model by requiring the stability of the scalar potential and the perturbativity of the couplings as they evolve with the renormalization scale. To this end, we consider the scalar couplings (except λ_h) and the gauge coupling g_X and generate random values inside the intervals shown below,

$$\lambda_1,\, \lambda_2,\, \lambda_3,\, \lambda_{h1},\, \lambda_{h2},\, \lambda_4,\, \lambda_5 \ \in\ \left[10^{-6}, 1\right], \quad g_X \ \in\ [0, 3]\,. \tag{3.7}$$

The scalar couplings are specified at the renormalization scale Λ where the tree-level potential is minimized, whereas the dark gauge coupling is defined at the scale of the lightest dark gauge boson $g_X(M_{X^{3'}})$.

Then, we calculate the VEVs v_1, v_2 and the Higgs self-coupling λ_h from the minimization conditions (2.10)–(2.13). At the first stage, we keep only the points that reproduce the measured Higgs mass $M_{h_1} = 125.09 \pm 0.24$ GeV. Subsequently, we solve numerically the two-loop RGEs (cf. Appendix B) and keep only the values of the couplings that remain perturbative up to the Planck scale and also satisfy the vacuum stability conditions (2.7)–(2.9), as well as the bound set by LHC (3.5) and the constraints on the parameters S and T (3.6). We present five of these benchmark points in Table 3.

Most of these benchmark points (BPs) contain values for the dark VEVs for which $v_1^2 \gg v_2^2$. This results in the masses of the dark gauge bosons X^1_μ, X^2_μ, $X^{3'}_\mu$ being nearly degenerate, while

	BP1	BP2	BP3	BP4	BP5
$\lambda_1\,(\Lambda)$	0.00008	0.0112	0.0014	0.00017	0.00015
$\lambda_2\,(\Lambda)$	0.0706	0.01073	0.0689	0.12129	0.00126
$\lambda_{h1}\,(\Lambda)$	0.00292	0.0237	0.00282	0.0006	0.0016
$\lambda_{h2}\,(\Lambda)$	0.04116	0.00323	0.00031	0.00109	0.00344
$\lambda_3\,(\Lambda)$	0.00459	0.0211	0.0196	0.00911	0.00088
$\lambda_4\,(\Lambda)$	0.3104	0.3317	0.2878	0.3363	0.3564
$\lambda_5\,(\Lambda)$	0.0052	0.000003	0.000011	0.13762	0.00167
$\lambda_h\,(\Lambda)$	0.13811	0.13201	0.12804	0.12876	0.13295
g_X	1.25	0.88	0.81	2.01	0.29
v_h	246.22	246.22	246.22	246.22	246.22
v_1	3180.05	882.78	2365.61	5272.32	6610.41
v_2	557.43	869.86	891.70	1021.43	3898.50
M_{h_1}	125.07	125.02	125.17	125.08	125.14
M_{h_2}	588.86	97.82	189.80	2500.34	227.22
M_{h_3}	215.81	184.42	353.78	512.43	228.37
$M_{\tilde{\phi}_3}$	1282.51	504.70	958.99	2614.19	3247.10
$M_{\tilde{\phi}_4}$	1261.21	504.69	958.95	1692.65	3231.93
$M_{X_{1,2}}$	349.65	382.29	361.14	1028.25	560.84
$M_{X'_3}$	348.29	314.41	354.20	1023.32	531.48
$M_{X_{4,5}}$	1994.73	387.97	958.07	5307.55	950.98
$M_{X_{6,7}}$	2025.14	544.67	1023.88	5406.23	1104.05
$M_{X'_8}$	2312.35	544.70	1127.97	6158.13	1158.77
Λ	1747.67	407.03	834.25	4704.95	1838.82
$\Omega_X h^2$	0.0365	0.0670	0.1136	0.0952	6.19
$\sigma^{\rm eff}_{1,2}$	2.2×10^{-45}	1.0×10^{-47}	1.5×10^{-47}	8.7×10^{-48}	0
$\sigma^{\rm eff}_{3}$	1.2×10^{-44}	7.7×10^{-46}	2.8×10^{-46}	5.5×10^{-47}	1.5×10^{-46}

Table 3: Benchmark points for the model parameters that satisfy the stability and perturbativity constraints, as well as the bounds set by LHC and measurements of the oblique parameters. The VEVs, the masses, and Λ are in GeV units. For completeness, we have also included the values of the total relic density of $X^{1,2,3'}$ and their effective scattering cross sections off a nucleon (in cm^2 units) which we discuss in Secs. 4.1 and 4.2.

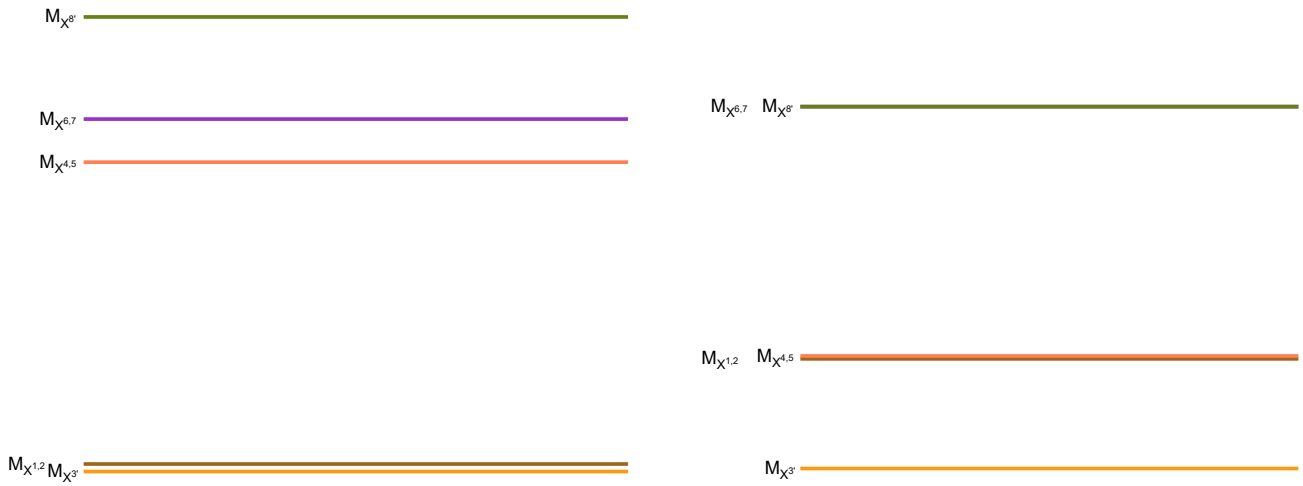

Figure 1: Mass spectra of dark gauge bosons for the cases $v_1^2 \gg v_2^2$ (left) and $v_1 \simeq v_2$ (right).

the masses of the rest of the dark gauge bosons are well above them. Nonetheless, in BP2, we have also included the case $v_1 \simeq v_2$. In this case, the mass of $X_\mu^{3'}$ is fairly lower than the masses of X_μ^1 and X_μ^2, which are now close to the masses of X_μ^4 and X_μ^5, while the masses of X_μ^6 and X_μ^7 become nearly degenerate with the mass of $X_\mu^{8'}$. Therefore, in the case $v_1 \simeq v_2$, we have

$$M_{X^{3'}}^2 \simeq \frac{2}{3} M_{X^{1,2}}^2 \simeq \frac{2}{3} M_{X^{4,5}}^2 \simeq \frac{1}{3} M_{X^{6,7}}^2 \simeq \frac{1}{3} M_{X^{8'}}^2 . \tag{3.8}$$

As we will see in the next section, the case $v_1 \simeq v_2$ is distinct in its dark matter analysis.

Regarding the scalar bosons and the pNGB h_2 in particular, we observe that its mass depends highly on the values of the VEVs v_1, v_2 and the dark gauge coupling g_X, or equivalently on the masses of the dark gauge bosons and the rest of the scalars [cf. (2.30)]. For example, large values for the VEVs and g_X produce a large mass for h_2, as can be seen from BP4 in Table 3.

Finally, the dark gauge boson mass spectrum for both cases $v_1^2 \gg v_2^2$ and $v_1 \simeq v_2$ is shown schematically in Fig. 1.

4. Dark matter analysis

Recent astrophysical measurements [112] have corroborated the now well-established fact that $\sim 80\%$ of the nonrelativistic matter in the Universe is in a form that remains a mystery to us and cannot be explained by the known particles and forces. This "dark matter" (DM) could be constituted of scalar bosons, fermions, vector bosons, a combination of the above, or even something more exotic. Here we will focus on vector DM [73, 74, 82, 92, 97, 103, 113–144].

Whatever the case may be, a DM candidate particle should be stabilized by some kind of symmetry, such that it may not decay to the SM particles. The simplest possibility of a stabilizing symmetry is that of a Z_2 discrete symmetry. A neutral and weakly interacting massive particle can be a DM candidate if it is the lightest Z_2-odd particle in a given model. In order to accommodate more DM candidates, one should consider a Z_N ($N \geq 4$) or a product of two or more Z_2's as the stabilizing symmetry.

The intrinsic $Z_2 \times Z_2'$ symmetry of the dark sector of the model, not shared by the SM fields, singles out the particles with nontrivial signatures under this symmetry as a stable sector without any other symmetry requirements. The lightest of the dark gauge bosons then, are possible dark matter candidates. Under our assumptions, the lightest of them are the dark gauge bosons X_μ^1, X_μ^2 and $X_\mu^{3'}$.

The present model allows for various processes that are able to change the number density of dark matter particles. These are the following:

(a) *Annihilation into SM.* All dark gauge bosons interact with the scalars h_i ($i = 1, 2, 3$), which in turn communicate with the SM fields. Thus, the DM candidates $X_\mu^{1,2,3'}$ can annihilate to the SM particles through the Higgs portal.

(b) *Semiannihilation.* The non-Abelian nature of the extra gauge symmetry allows the processes $X^a X^b \to X^c h_i$ to occur. In this case, the final number of DM particles is one less than the initial number, as opposed to the case of annihilations where the DM number of particles is changed by two units. Semiannihilation processes are of great interest regarding DM phenomenology since they can dominate in much of the parameter space.

(c) *Coannihilation.* This kind of process has been thoroughly investigated in the context of supersymmetric DM models.[3] There, the lightest neutralino particle (LSP) is a DM candidate and can potentially coannihilate with the next-to-lightest supersymmetric particle (NLSP) if their respective masses are close enough. A similar situation arises in the dark sector of the model under consideration when $v_1 \simeq v_2$, since in that case the masses of the DM candidates X_μ^1 and X_μ^2 are close to those of X_μ^4 and X_μ^5 (cf. Fig. 1) and may in principle coannihilate with them through the processes $X^1 X^{4,5} \to X^{7,6} h_i$ and $X^2 X^{4,5} \to X^{6,7} h_i$. Notice, however, that we cannot employ the usual condition between the LSP and NLSP(s) number densities before, during, and after freeze-out, namely $n_i/n_j = n_i^{eq}/n_j^{eq}$, since its validity cannot be guaranteed when semiannihilations are also involved (see Ref. [146] for more details).

(d) *DM conversion.* In multicomponent DM systems the various DM candidates have different masses in general. Then, if the relevant interactions are allowed, a DM species may be converted to another. In this model the three DM candidates $X_\mu^{1,2,3'}$ are nearly degenerate in mass, and such processes $\left(X^{1,2} X^{1,2} \to X^{3'} X^{3'}\right)$ are generally phase space suppressed. However, again in the limiting case $v_1 \simeq v_2$ the mass splitting of $X_\mu^{3'}$ with regard to X_μ^1 and X_μ^2 can have a significant effect in today's number density of these DM species.

[3] See, for example, Ref. [145] and references therein.

4.1. Boltzmann equations and relic density

In order to determine the present day abundance of the DM species we need to solve a coupled set of Boltzmann equations involving the number densities of the dark sector particles. These equations can be written in a compact form as

$$\frac{dn_a}{dt} + 3H\, n_a = \mathcal{C}_a \qquad (a = 1, 2, 3')\,, \tag{4.1}$$

with H being the Hubble parameter and $\mathcal{C}_a = \sum_{bcd} \mathcal{C}_{ab\to cd}$ being the collision rate of all possible $2 \to 2$ processes for a given species that can change its number density. We can relate the collision rate of a reaction with its inverse by making use of the detailed balance equation

$$\mathcal{C}_{ab\to cd} = -\langle\sigma_{ab\to cd} v_r\rangle \left(n_a n_b - n_c n_d \frac{\bar{n}_a \bar{n}_b}{\bar{n}_c \bar{n}_d}\right) = +\langle\sigma_{cd\to ab} v_r\rangle \left(n_c n_d - n_a n_b \frac{\bar{n}_c \bar{n}_d}{\bar{n}_a \bar{n}_b}\right)\,, \tag{4.2}$$

where $\bar{n} \equiv n^{\rm eq}$ is the equilibrium number density and $\langle\sigma_{ab\to cd} v_r\rangle$ is the thermally averaged cross section times the relative velocity of the DM particles. It is given by the general formula [147–149]

$$\langle\sigma_{ab\to cd} v_r\rangle = \frac{1}{2m_a^2 m_b^2 T K_2(m_a/T) K_2(m_b/T)} \int_{(m_a+m_b)^2}^{\infty} ds K_1(\sqrt{s}/T) p_{\rm in}(s) w(s), \tag{4.3}$$

where $w(s) = E_a E_b \sigma_{ab\to cd} v_r$. The cross section for a given process $a + b \to c + d$ is

$$\sigma_{ab\to cd} v_r = \frac{1}{1+\delta_{cd}} \frac{p_{\rm out}(s)}{32\pi s p_{\rm in}(s)} \int d\cos\theta\, |\mathcal{M}_{ab\to cd}|^2\,, \tag{4.4}$$

with $|\mathcal{M}|^2$ denoting the spin summed and polarization averaged matrix element squared. In Eq. (4.3), $K_\nu(z)$ stands for the modified Bessel functions. The general expressions for the kinematical variables contained in (4.3) and (4.4) are provided in Appendix C.

We may now proceed to obtain the relic abundance of the DM candidates by solving numerically the set of Boltzmann equations. In order to write down the system of coupled equations, we need to identify the reactions which modify the number of X^1_μ, X^2_μ, and $X^{3'}_\mu$ particles. Since $M_{X_1} = M_{X_2} > M_{X_{3'}}$, the number densities satisfy $n_1 = n_2 \neq n_3$. It should also be clear that $\langle\sigma v_r\rangle_{11\to\chi\chi'} = \langle\sigma v_r\rangle_{22\to\chi\chi'} \neq \langle\sigma v_r\rangle_{33\to\chi\chi'}$, $\langle\sigma v_r\rangle_{12\to 3\chi} = \langle\sigma v_r\rangle_{21\to 3\chi} \neq \langle\sigma v_r\rangle_{13\to 2\chi} = \langle\sigma v_r\rangle_{31\to 2\chi} = \langle\sigma v_r\rangle_{23\to 1\chi} = \langle\sigma v_r\rangle_{32\to 1\chi}$, and $\langle\sigma v_r\rangle_{11\to 33} = \langle\sigma v_r\rangle_{22\to 33} \neq \langle\sigma v_r\rangle_{33\to 11} = \langle\sigma v_r\rangle_{33\to 22}$, where, for example, $\langle\sigma v_r\rangle_{12\to 3\chi}$ is short for $\langle\sigma v_r\rangle_{X_1 X_2\to X_{3'}\chi}$, etc., and $\chi\chi'$ denotes SM SM and $h_i h_j$ pairs when these are kinematically allowed.

The processes which modify the number of $X^{1,2}_\mu$ particles are

$$X^{1,2}X^{1,2} \to \chi\chi', \qquad X^{1,2}X^{2,1} \to X^{3',8'}h_i, \qquad X^{1,2}X^{3'} \to X^{2,1}h_i, \qquad X^{1,2}X^{1,2} \to X^{3'}X^{3'}, \tag{4.5}$$

whereas the ones which modify the number of $X^{3'}$ particles are

$$X^{3'}X^{3'} \to \chi\chi', \qquad X^{1,2}X^{3'} \to X^{2,1}h_i, \qquad X^{3'}h_i \to X^{1,2}X^{2,1}, \qquad X^{3'}X^{3'} \to X^{1,2}X^{1,2}. \tag{4.6}$$

The collision operators for the processes which modify the number of X^1_μ and X^2_μ particles are

$$\begin{aligned}
\mathcal{C}_{11\to\chi\chi'} &= -\langle\sigma v_r\rangle_{11\to\chi\chi'}\left[n_1^2-\overline{n}_1^2\right] = \mathcal{C}_{22\to\chi\chi'},\\
\mathcal{C}_{12\to 3h_i} &= -\langle\sigma v_r\rangle_{12\to 3h_i}\left[n_1n_2-\overline{n}_1\overline{n}_2\frac{n_3}{\overline{n}_3}\right] = \mathcal{C}_{21\to 3h_i},\\
\mathcal{C}_{12\to 8h_i} &= -\langle\sigma v_r\rangle_{12\to 8h_i}\left[n_1n_2-\overline{n}_1\overline{n}_2\right] = \mathcal{C}_{21\to 8h_i},\\
\mathcal{C}_{13\to 2h_i} &= -\langle\sigma v_r\rangle_{13\to 2h_i}\left[n_1n_3-\overline{n}_1\overline{n}_3\frac{n_2}{\overline{n}_2}\right] = \mathcal{C}_{23\to 1h_i},\\
\mathcal{C}_{11\to 33} &= -\langle\sigma v_r\rangle_{11\to 33}\left[n_1^2-n_3^2\frac{\overline{n}_1^2}{\overline{n}_3^2}\right] = \mathcal{C}_{22\to 33},\\
\mathcal{C}_{1h_i\to 23} &= +\langle\sigma v_r\rangle_{23\to 1h_i}\left[n_2n_3-\overline{n}_2\overline{n}_3\frac{n_1}{\overline{n}_1}\right] = \mathcal{C}_{2h_i\to 13},
\end{aligned} \tag{4.7}$$

whereas the ones which modify the number of $X^{3'}_\mu$ particles are

$$\begin{aligned}
\mathcal{C}_{33\to\chi\chi'} &= -\langle\sigma v_r\rangle_{33\to\chi\chi'}\left[n_3^2-\overline{n}_3^2\right],\\
\mathcal{C}_{13\to 2h_i} &= -\langle\sigma v_r\rangle_{13\to 2h_i}\left[n_1n_3-\overline{n}_1\overline{n}_3\frac{n_2}{\overline{n}_2}\right] = \mathcal{C}_{23\to 1h_i},\\
\mathcal{C}_{33\to 11} &= +\langle\sigma v_r\rangle_{11\to 33}\left[n_1^2-n_3^2\frac{\overline{n}_1^2}{\overline{n}_3^2}\right] = \mathcal{C}_{33\to 22},\\
\mathcal{C}_{3h_i\to 12} &= +\langle\sigma v_r\rangle_{12\to 3h_i}\left[n_1n_2-\overline{n}_1\overline{n}_2\frac{n_3}{\overline{n}_3}\right].
\end{aligned} \tag{4.8}$$

As discussed above, in the case $v_1 \simeq v_2$, the particles $X^{4,5}_\mu$ are thermally available to $X^{1,2}_\mu$ and may coannihilate with them. We therefore also have to include them in our analysis. The collision operators for the processes which change the number of $X^{4,5}_\mu$ particles are[4]

[4]Of course, these reactions also change the number of $X^{1,2,3'}_\mu$ particles. Also, we have assumed that the heavier dark gauge bosons $X^{6,7,8'}_\mu$ have already decayed to the lighter ones.

$$
\begin{aligned}
\mathcal{C}_{44\to\chi\chi'} &= -\left\langle\sigma v_r\right\rangle_{44\to\chi\chi'}\left[n_4^2-\overline{n}_4^2\right]=\mathcal{C}_{55\to\chi\chi'},\\
\mathcal{C}_{14\to 7h_i} &= -\left\langle\sigma v_r\right\rangle_{14\to 7h_i}\left[n_1 n_4-\overline{n}_1\overline{n}_4\right]=\mathcal{C}_{15\to 6h_i}=\mathcal{C}_{24\to 6h_i}=\mathcal{C}_{25\to 7h_i},\\
\mathcal{C}_{44\to 11} &= -\left\langle\sigma v_r\right\rangle_{44\to 11}\left[n_4^2-n_1^2\frac{\overline{n}_4^2}{\overline{n}_1^2}\right]=\mathcal{C}_{44\to 22}=\mathcal{C}_{55\to 11}=\mathcal{C}_{55\to 22},\\
\mathcal{C}_{44\to 33} &= -\left\langle\sigma v_r\right\rangle_{44\to 33}\left[n_4^2-n_3^2\frac{\overline{n}_4^2}{\overline{n}_3^2}\right]=\mathcal{C}_{55\to 33}
\end{aligned}
\tag{4.9}
$$

Next, let us define

$$
Y_a\equiv\frac{n_a}{s},\qquad x\equiv\frac{M_{X^{3'}}}{T},\qquad \mathcal{Z}_{ab\to cd}(x)\equiv\frac{s(x=1)}{H(x=1)}\langle\sigma v_r\rangle_{ab\to cd}\,,
\tag{4.10}
$$

where $H=\sqrt{\frac{4\pi^3 g_\star}{45}}\,\frac{T^2}{M_{\rm Pl}}$, $g_\star\simeq g_{\star s}$ is the number of effective relativistic degrees of freedom, and $s=\frac{2\pi^2 g_{\star s}}{45}\,T^3$ is the entropy density. Then, we may finally write down the coupled set of Boltzmann equations in dimensionless variables as

$$
\begin{aligned}
\frac{dY_1}{dx}=-\frac{1}{x^2}\Bigg\{&\mathcal{Z}_{11\to\chi\chi'}\left[Y_1^2-\overline{Y}_1^2\right]+\mathcal{Z}_{12\to 3h_i}\left[Y_1Y_2-\overline{Y}_1\overline{Y}_2\frac{Y_3}{\overline{Y}_3}\right]\\
&+\mathcal{Z}_{12\to 8h_i}\left[Y_1Y_2-\overline{Y}_1\overline{Y}_2\right]+\mathcal{Z}_{13\to 2h_i}\left[Y_1Y_3-\overline{Y}_1\overline{Y}_3\frac{Y_2}{\overline{Y}_2}\right]\\
&-\mathcal{Z}_{23\to 1h_i}\left[Y_2Y_3-\overline{Y}_2\overline{Y}_3\frac{Y_1}{\overline{Y}_1}\right]+\mathcal{Z}_{11\to 33}\left[Y_1^2-Y_3^2\frac{\overline{Y}_1^2}{\overline{Y}_3^2}\right]\\
&-\mathcal{Z}_{44\to 11}\left[Y_4^2-Y_1^2\frac{\overline{Y}_4^2}{\overline{Y}_1^2}\right]-\mathcal{Z}_{55\to 11}\left[Y_5^2-Y_1^2\frac{\overline{Y}_5^2}{\overline{Y}_1^2}\right]\\
&+\mathcal{Z}_{14\to 7h_i}\left[Y_1Y_4-\overline{Y}_1\overline{Y}_4\right]+\mathcal{Z}_{15\to 6h_i}\left[Y_1Y_5-\overline{Y}_1\overline{Y}_5\right]\Bigg\}\,,
\end{aligned}
\tag{4.11}
$$

$$
\frac{dY_2}{dx}=\frac{dY_1}{dx}(1\leftrightarrow 2,4\leftrightarrow 5,7\leftrightarrow 6)
\tag{4.12}
$$

$$\frac{dY_3}{dx} = -\frac{1}{x^2}\left\{\mathcal{Z}_{33\to\chi\chi'}\left[Y_3^2-\overline{Y}_3^2\right]+\mathcal{Z}_{13\to 2h_i}\left[Y_1Y_3-\overline{Y}_1\overline{Y}_3\frac{Y_2}{\overline{Y}_2}\right]\right.$$
$$+\mathcal{Z}_{23\to 1h_i}\left[Y_2Y_3-\overline{Y}_2\overline{Y}_3\frac{Y_1}{\overline{Y}_1}\right]-\mathcal{Z}_{11\to 33}\left[Y_1^2-Y_3^2\frac{\overline{Y}_1^2}{\overline{Y}_3^2}\right]$$
$$-\mathcal{Z}_{22\to 33}\left[Y_2^2-Y_3^2\frac{\overline{Y}_2^2}{\overline{Y}_3^2}\right]-\mathcal{Z}_{44\to 33}\left[Y_4^2-Y_3^2\frac{\overline{Y}_4^2}{\overline{Y}_3^2}\right] \tag{4.13}$$
$$\left.-\mathcal{Z}_{55\to 33}\left[Y_5^2-Y_3^2\frac{\overline{Y}_5^2}{\overline{Y}_3^2}\right]-2\,\mathcal{Z}_{12\to 3h_i}\left[Y_1Y_2-\overline{Y}_1\overline{Y}_2\frac{Y_3}{\overline{Y}_3}\right]\right\}.$$

$$\frac{dY_4}{dx} = -\frac{1}{x^2}\left\{\mathcal{Z}_{44\to\chi\chi'}\left[Y_4^2-\overline{Y}_4^2\right]+\mathcal{Z}_{44\to 11}\left[Y_4^2-Y_1^2\frac{\overline{Y}_4^2}{\overline{Y}_1^2}\right]\right.$$
$$+\mathcal{Z}_{44\to 22}\left[Y_4^2-Y_2^2\frac{\overline{Y}_4^2}{\overline{Y}_2^2}\right]+\mathcal{Z}_{44\to 33}\left[Y_4^2-Y_3^2\frac{\overline{Y}_4^2}{\overline{Y}_3^2}\right] \tag{4.14}$$
$$\left.+\mathcal{Z}_{14\to 7h_i}\left[Y_1Y_4-\overline{Y}_1\overline{Y}_4\right]+\mathcal{Z}_{24\to 6h_i}\left[Y_2Y_4-\overline{Y}_2\overline{Y}_4\right]\right\},$$

$$\frac{dY_5}{dx} = \frac{dY_4}{dx}(4\leftrightarrow 5, 1\leftrightarrow 2, 7\leftrightarrow 6). \tag{4.15}$$

The equilibrium yields $\overline{Y}_a \equiv \frac{\overline{n}_a}{s}$ are given by

$$\overline{Y}_3 = \frac{\hat{g}_X}{g_{\star s}}\frac{45}{4\pi^4}x^2K_2(x), \tag{4.16}$$
$$\overline{Y}_{1,2} = \frac{\hat{g}_X}{g_{\star s}}\frac{45}{4\pi^4}r_{1,2}^2x^2K_2(r_{1,2}x), \tag{4.17}$$
$$\overline{Y}_{4,5} = \frac{\hat{g}_X}{g_{\star s}}\frac{45}{4\pi^4}r_{4,5}^2x^2K_2(r_{4,5}x), \tag{4.18}$$

where we have defined $r_{1,2}\equiv\frac{M_{X^{1,2}}}{M_{X^{3'}}}$, $r_{4,5}\equiv\frac{M_{X^{4,5}}}{M_{X^{3'}}}$ and $\hat{g}_X=3$ are the spin degrees of freedom of the dark gauge bosons. We have numerically solved this system using `Mathematica` and we have also employed the packages `FeynArts/FormCalc` [150, 151] in order to produce analytic results for the various cross sections involved. Finally, we have obtained the total relic density of the $X_\mu^{1,2,3'}$ particles

$$\Omega_X h^2 = \Omega_{X^1}h^2+\Omega_{X^2}h^2+\Omega_{X^{3'}}h^2, \tag{4.19}$$

where

$$\Omega_{X^a}h^2 = \frac{M_{X^a}s_0Y^a(\infty)}{\rho_c/h^2}, \tag{4.20}$$

with $s_0 = 2890\ \text{cm}^{-3}$ and $\rho_c/h^2 = 1.05 \times 10^{-5}\ \text{GeV/cm}^3$. Equation (4.19) has to be compared with the measured DM relic density $\Omega_{\rm DM}h^2 = 0.1197 \pm 0.0022$ [112]. Next, we further explore the cases $v_1^2 \gg v_2^2$ and $v_1 \simeq v_2$.

4.1.1. Case $v_1^2 \gg v_2^2$

In this case, as stated above, the masses of the DM candidates X^1, X^2, and $X^{3'}$ are nearly degenerate, while the masses of X^4 and X^5 are well above those of X^1 and X^2. Therefore, coannihilation effects play no significant role in the final relic density of $X^{1,2,3'}$. However, even though the mass splitting between $M_{X^1} = M_{X^2}$ and $M_{X^{3'}}$ is small, the DM conversion processes $X^{1,2}X^{1,2} \to X^{3'}X^{3'}$ can lower the number density of X^1 and X^2 and enhance that of $X^{3'}$, rendering $X^{3'}$ the predominant DM component.

To get a feeling of the effect of DM conversion, we set the parameters of the model according to BP1 of Table 3 and solve numerically the Boltzmann equations (4.11)–(4.13) (omitting the coannihilation terms), thus obtaining the solutions for the yields $Y_{1,2}$ and Y_3 with respect to $x = M_{X^{3'}}/T$.

In Fig. 2 we plot these solutions with the DM conversion processes switched on (left) and switched off (right). When the DM conversion is switched off, the final yields are closer together, with the separation attributed to the slightly different masses between $X^{1,2}$ and $X^{3'}$, as well as to the mixing between $X^{3'} - X^{8'}$ which results in more Feynman diagrams contributing to the annihilation processes $X^{3'}X^{3'} \to h_i h_j$ and the semiannihilation processes $X^{1,2}X^{2,1} \to X^{3'}h_i$.[5] On the other hand, the separation of the final yields is larger when the DM conversion processes are switched on, since more X^1 and X^2 particles have annihilated and have been converted to $X^{3'}$; a reaction that continues to occur to some extent even after freeze-out. In the case without DM conversion, the particles X^1, X^2, and $X^{3'}$ comprise 19%, 19%, and 62% of the total relic density respectively, while in the case with DM conversion they comprise 13%, 13%, and 74% of the total relic density, respectively.

In Fig. 3 we fix again the model parameters as in BP1, but this time we leave the extra gauge coupling g_X free and scan over it, ergo obtaining the total relic density $\Omega_X h^2$ of the DM candidates. We first observe a resonant dip around 110 GeV which corresponds to $M_{X^{3'}} \simeq M_{X^{1,2}} = M_{h_3}/2$. Then the relic density grows until ~ 175 GeV where the $t\bar{t}$ channel opens up. After that, there is a steep decrease around $M_{h_3} \simeq 215$ GeV where all the annihilation channels $X^aX^a \to h_3h_3$ and the semiannihilation channels $X^aX^b \to X^ch_3$ become kinematically available. This point crosses the observed DM relic density (blue band in Fig. 3) and corresponds to $g_X = 0.78$ (which also

[5] In the non-CSI version of this model considered in Ref. [103], the authors performed their $SU(3)$ DM analysis under the simplified assumption that the rest of the dark sector particles do not contribute to DM annihilation. They also only included the couplings of the DM candidates to the two lightest scalar bosons h_1, h_2 and not the heavier $\mathcal{H}$ in their notation. Here, we include all possible couplings and Feynman diagrams relevant to the relic densities of $X^{1,2,3'}$.

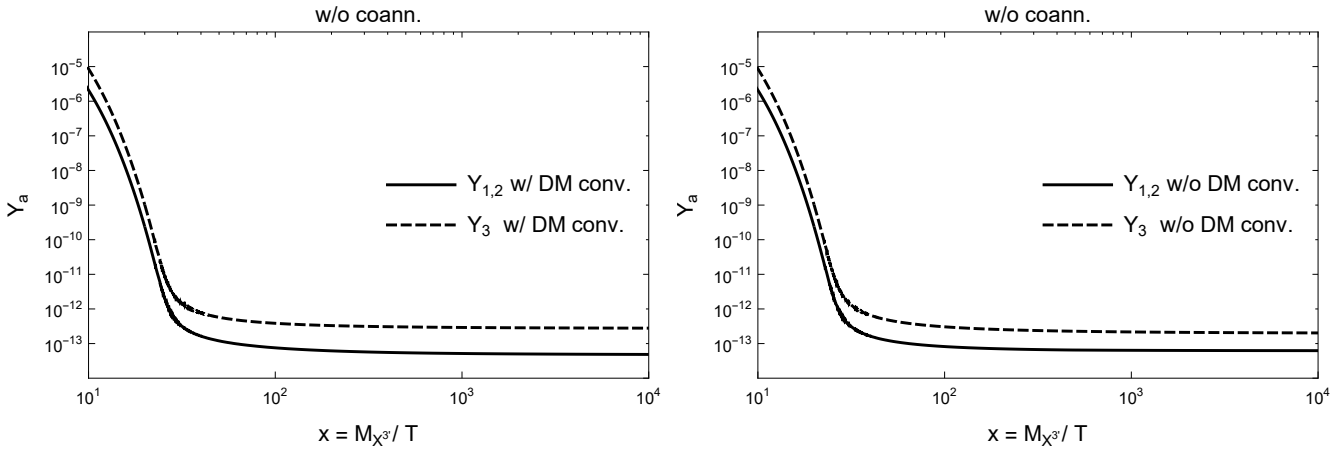

Figure 2: The yields $Y_{1,2}$ and Y_3 in terms of $x = M_{X^{3'}}/T$ for BP1. The right plot has been obtained neglecting the DM conversion terms in the Boltzmann equations. These terms are included in the left plot. The DM conversion process reduces the final number density of the X^1 and X^2 particles since some of them are converted to $X^{3'}$.

satisfies the constraints discussed in Sec. 3).

Above M_{h_3}, one may expect that the relic density would decrease monotonically. This can be understood as follows: every vertex containing three dark gauge boson legs is proportional to g_X while every vertex containing two dark gauge bosons and one or two scalar bosons is proportional to g_X^2. Therefore, $\langle \sigma v_r \rangle \propto g_X^2$, or $\Omega_X h^2 \propto 1/g_X^2$. This indicates that the relic density should decrease as we increase g_X (and therefore $M_{X^{1,2,3'}}$). Nevertheless, the mass of the pNGB M_{h_2} depends on all the masses of the model [cf. (2.30)]. This means that as g_X grows, so do the dark gauge boson masses and consequently M_{h_2}. This effect tends to counterbalance the expected decrease of $\Omega_X h^2$. On the other hand, as g_X becomes smaller, the relic density of the DM candidates increases considerably and tends to overclose the Universe. For example, the small value of g_X from BP5 in Table 3 leads to $\Omega_X h^2 \simeq 6.2$, in which case $X^{1,2}$ are also completely depleted and $X^{3'}$ makes up 100% of the relic density. Furthermore, the dependence of M_{h_2} on g_X means that there can be only two resonant dips, corresponding to $M_{h_1}/2$ and $M_{h_3}/2$. This is in contrast to the non-CSI version of the model [103] where there should be three resonant dips, corresponding to $M_{h_1}/2$, $M_{h_2}/2$, $M_{h_3}/2$, since in that case M_{h_2} does not depend on g_X. As a result, the CSI version of the model that we consider is in general more constrained.

4.1.2. Case $v_1 \simeq v_2$

In this case, $X^{3'}$ is nearly 20% lighter than X^1 and X^2 [cf. (3.8)] while X^4 and X^5 are almost degenerate with the latter ones. Therefore, coannihilations between $X^{1,2}$ and $X^{4,5}$ may occur around the time of freeze-out and influence the relic density of these four particles. Since the

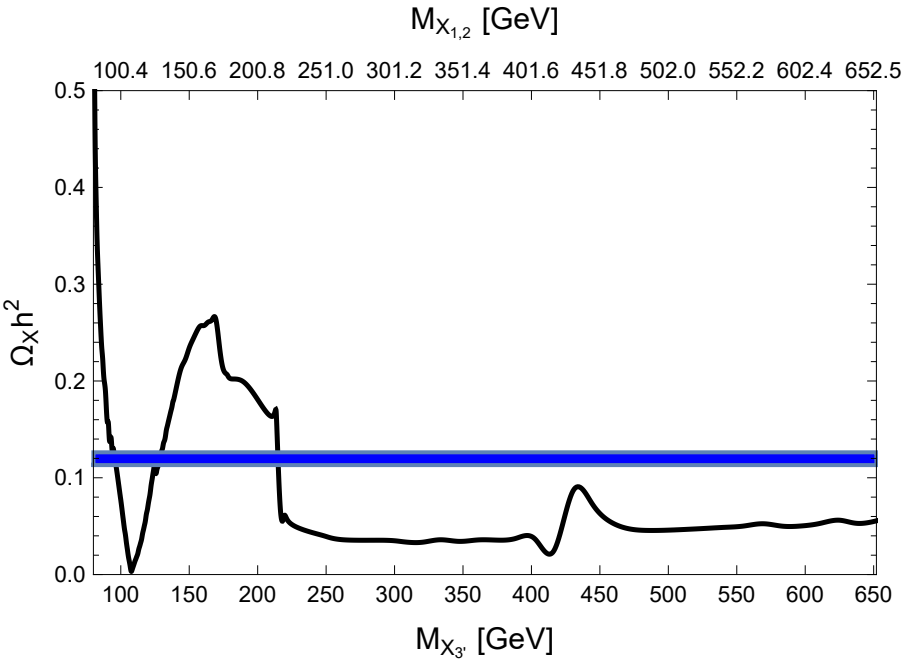

Figure 3: The total relic density of $X^{1,2}$ and $X^{3'}$ as a function of the dark gauge coupling g_X for BP1. The blue band corresponds to the observed DM relic density within 3σ.

semiannihilations $X^{1,2}X^{3'} \to X^{2,1}h_i$ are now phase-space suppressed, the Boltzmann equations governing the number densities of $X^{1,2}$ and $X^{4,5}$ are almost identical. We therefore expect their relic number densities to be very close. This is indeed the case as can be seen in Fig. 4.

There, we also distinguish between the cases when coannihilations are switched on (left) and switched off (right). The effect is clearly insignificant, and in both cases the DM candidates X^1, X^2, and $X^{3'}$ comprise approximately 1%, 1%, and 98% of the total relic density, respectively. The dominant phenomenon is DM conversion since most $X^{1,2}$ and $X^{4,5}$ have had enough time to annihilate to $X^{3'}$.

We display the importance of this effect in Fig. 5, where coannihilations are switched on, but this time we distinguish between the cases when DM conversion is switched on (left) and off (right). With DM conversion switched on, the DM candidates X^1, X^2, and $X^{3'}$ comprise again 1%, 1%, and 98% of the total relic density. With DM conversion switched off, X^1, X^2, and $X^{3'}$ comprise around 7%, 7%, and 86% of the total relic density, respectively. Moreover, the total relic density is almost 2 times larger in the former case (DM conversion on) than in the latter case (DM conversion off). This can be attributed to the fact that without DM conversion freeze-out is delayed and more DM particles have time to annihilate to SM particles.

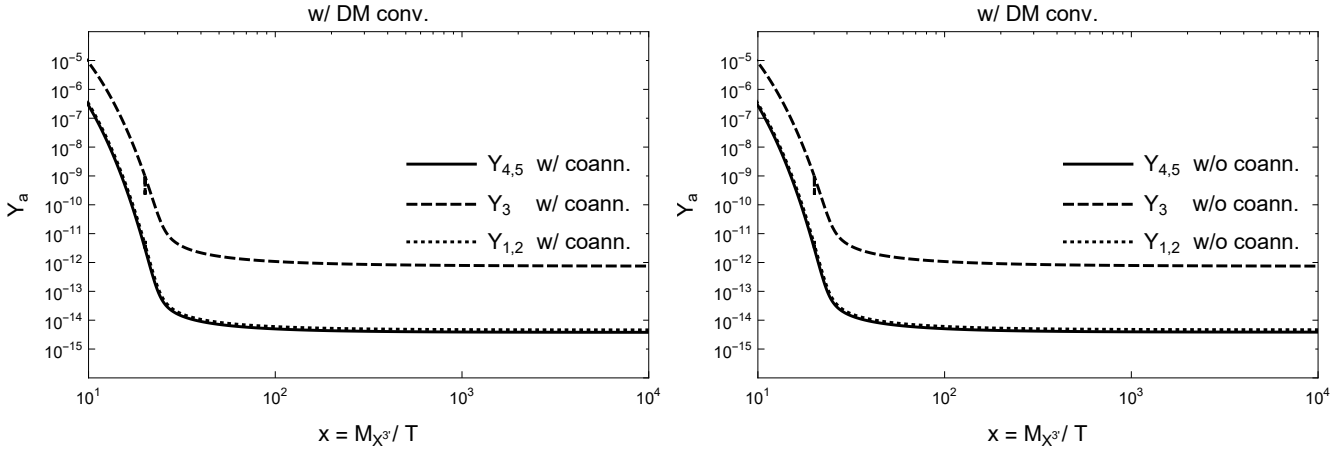

Figure 4: The yields $Y_{1,2}$, Y_3, and $Y_{4,5}$ in terms of $x = M_{X^{3'}}/T$ for BP2. The right plot has been obtained neglecting the coannihilation terms in the Boltzmann equations. These terms are included in the left plot. The difference is very small since most $X^{1,2}$ and $X^{4,5}$ particles are converted to $X^{3'}$.

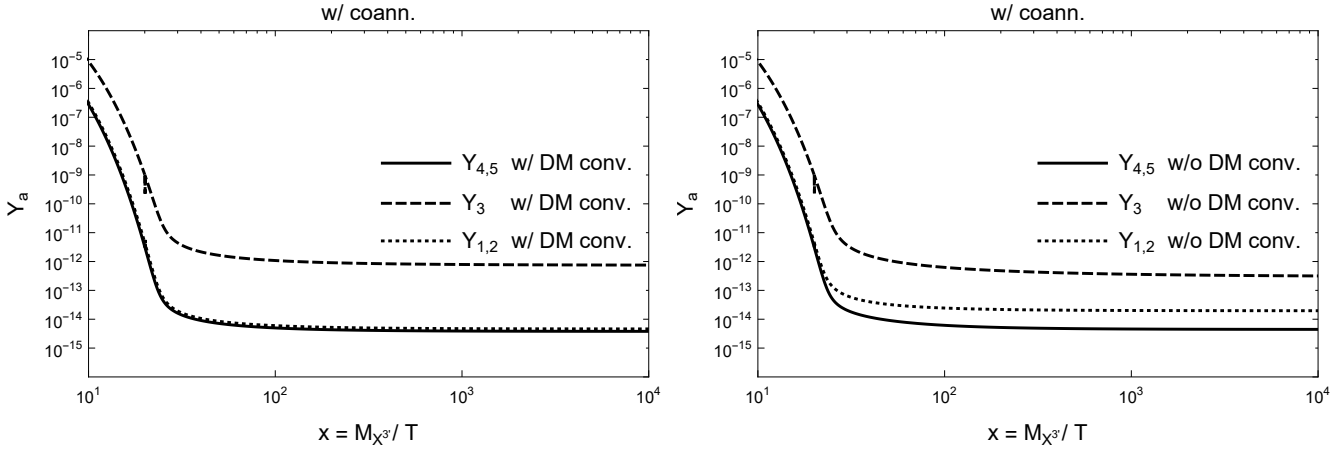

Figure 5: The yields $Y_{1,2}$, Y_3, and $Y_{4,5}$ in terms of $x = M_{X^{3'}}/T$ for BP2. The right plot has been obtained neglecting the DM conversion terms in the Boltzmann equations. These terms are included in the left plot. The DM conversion processes are significant since many $X^{1,2}$ particles are converted to $X^{3'}$.

4.2. Direct detection

Maybe the best prospect for validating the WIMP DM paradigm is through the direct detection of DM particles at deep underground facilities. Many experiments are in progress, and hopefully we may soon get a glimpse of this dark world.

Interactions between the DM particles $X_\mu^{1,2,3'}$ and the nucleons N can be mediated through a t-channel exchange of the scalar bosons h_i. For the individual DM components, the corresponding spin-independent elastic scattering cross sections are

$$\sigma_{1,2}^{\rm SI} = \frac{f_N^2}{16\pi v_h^2}\frac{m_N^4}{\left(M_{X^{1,2}}+m_N\right)^2}\left|g_X^2 v_2\sum_{i=1}^{3}\frac{\mathcal{R}_{i3}\mathcal{R}_{1i}}{M_{h_i}^2}\right|^2, \tag{4.21}$$

$$\begin{aligned}\sigma_3^{\rm SI} = \frac{f_N^2}{16\pi v_h^2}\frac{m_N^4}{\left(M_{X^{3'}}+m_N\right)^2}\Bigg|&\frac{4}{3}g_X^2 v_1\sin^2\delta\sum_{i=1}^{3}\frac{\mathcal{R}_{i2}\mathcal{R}_{1i}}{M_{h_i}^2}\\ &+\frac{1}{3}g_X^2 v_2\left(\cos 2\delta+2-\sqrt{3}\sin 2\delta\right)\sum_{i=1}^{3}\frac{\mathcal{R}_{i3}\mathcal{R}_{1i}}{M_{h_i}^2}\Bigg|^2,\end{aligned} \tag{4.22}$$

where $f_N \simeq 0.3$ [152–158] is the nucleon form factor and $m_N = 0.939$ GeV is the average nucleon mass.

Since we have three DM candidates with different masses ($M_{X^1} = M_{X^2} > M_{X^{3'}}$), not all of them contribute equally to the local DM density which in direct detection experiments is assumed to be composed of a single DM species. Nevertheless, we may assume that the contribution of each DM species to the local density is equal to the contribution of that particular species to the relic density and consequently construct the effective cross sections [159–161]

$$\sigma_a^{\rm eff} = \sigma_a^{\rm SI}\left(\frac{\Omega_{X^a}h^2}{\Omega_X h^2}\right). \tag{4.23}$$

For example, BP3 in Table 3 reproduces the observed DM relic density within 3σ, with X^1, X^2, and $X^{3'}$ comprising approximately 5%, 5%, and 90% of its total. The resulting effective cross sections are then

$$\begin{aligned}\sigma_{1,2}^{\rm eff} &= 1.46715\times10^{-47}\ {\rm cm}^2,\\ \sigma_3^{\rm eff} &= 2.77662\times10^{-46}\ {\rm cm}^2.\end{aligned}$$

Both of these numbers are well below the limits set by the LUX experiment [162], but are nevertheless within the reach of future experiments such as LZ [163] and XENON1T [164].

5. Summary and conclusions

In the present article we have examined a classically scale-invariant extension of the SM, enlarged by a weakly coupled dark $SU(3)_X$ gauge group. The extra sector consists of the eight dark gauge bosons and two complex scalar triplets. Under mild assumptions on the parameters of the scalar potential of the model the scalar triplets can develop nonvanishing VEVs and break the extra $SU(3)_X$ completely via the Coleman-Weinberg mechanism. Eight of the 12 scalar degrees of freedom are absorbed by the dark gauge bosons, rendering them all massive. We focused on and analyzed the case in which the symmetry breaking pattern involves two VEVs. As a result of the portal couplings of the dark scalars to the Higgs field, the dark gauge symmetry breakdown triggers electroweak symmetry breaking. In the framework of the Gildener-Weinberg formalism we considered the full one-loop effective potential. At one-loop level the pseudo–Nambu-Goldstone boson of broken classical scale symmetry receives a large radiative mass. Out of the massive dark gauge bosons the lightest three of them are almost degenerate in mass and also stable due to an intrinsic $Z_2 \times Z_2'$ discrete symmetry of $SU(3)_X$. These are identified as DM candidates.

The parameters of the model and the mass patterns resulting from symmetry breaking have subsequently been subjected to the various existing theoretical and experimental constraints. The requirements on the tree-level and one-loop effective scalar potential to be bounded from below have been analyzed. Constraints arising from LHC searches and measurements of the electroweak parameters S and T have also been examined. Thus, we obtained five benchmark points for the parameters of the model that stabilize the vacuum, satisfy the experimental constraints, and reproduce the measured mass for the observed Higgs boson.

Having analyzed the phenomenological viability of the model, a comprehensive DM analysis was undertaken. After identifying the relevant DM processes (annihilations, semiannihilations, coannihilations, and DM conversions), the set of coupled Boltzmann equations was constructed, describing the number density evolution of the DM candidates in order to obtain their total relic density and compare it to the measured value. The Boltzmann equations were solved numerically in two cases defined by the VEVs of the $SU(3)_X$ scalar fields.

In the first case, the VEV separation was large ($v_1^2 \gg v_2^2$) and the three dark gauge boson candidates X^1, X^2, and $X^{3'}$ were nearly degenerate in mass. This case may seem similar to the dark $SU(2)_X$ model (recently considered in Refs. [92] and [73, 74, 100, 142]) where the extra gauge symmetry gets broken by a complex scalar doublet. There, the three dark gauge bosons are completely degenerate in mass and contribute equally to the DM relic density. In the $SU(3)_X$ model, however, even though $X^{1,2,3'}$ are nearly degenerate in mass, the lightest of the three ($X^{3'}$) is the predominant DM component. This occurs mainly due to the mixing between $X^{3'}$ and $X^{8'}$ which means that more Feynman diagrams contribute to the semiannihilation processes $X^{1,2}X^{1,2} \to X^{3'}h_i$ and the annihilation processes $X^{3'}X^{3'} \to h_ih_j$. Also, even though the mass splitting is small, some of the $X^{1,2}$ particles are converted to $X^{3'}$ and increase its final relic density. Finally, as it is transparent in the framework of the GW formalism employed, the pNGB mass depends on all the other masses of the model. Consequently, there can be only one resonant dip for the

DM relic density in the $SU(2)_X$ model (corresponding to $M_{\rm Higgs}/2$) and two in the $SU(3)_X$ model (corresponding to $M_{h_1}/2$ and $M_{h_3}/2$). Therefore, in general, enlarging the gauge group means that more scalars are needed in order to break it, which leads to a larger parameter space that may be compatible with cosmological observations.

In the second case, the VEVs were very close ($v_1 \simeq v_2$). This resulted in $X^{3'}$ being around 20% lighter than X^1, X^2 (which were exactly degenerate) and X^4, X^5 (which were exactly degenerate too) now being close in mass with X^1 and X^2. Therefore, possible coannihilation effects had to be examined. Nevertheless, it turned out that the dominant process was DM conversion and $X^{3'}$ was again the predominant DM component. Finally, we determined that the DM candidates have viable prospects of being directly detected by future underground experiments.

Acknowledgements

A.K. would like to thank Dimitrios Karamitros for useful discussions. K.T. thanks the CERN Theory Division for its hospitality during the period when this work was completed.

A. Oblique Parameters

The S and T parameters are given in this model by the expressions (see also [34, 113, 138])

$$\begin{aligned} S &= \frac{1}{24\pi}\Bigg\{\mathcal{R}_{11}^2\left[\log R_{h_1 h} + G(M_{h_1}^2, M_Z^2) - G(M_h^2, M_Z^2)\right] \\ &\quad + \mathcal{R}_{12}^2\left[\log R_{h_2 h} + G(M_{h_2}^2, M_Z^2) - G(M_h^2, M_Z^2)\right] \\ &\quad + \mathcal{R}_{13}^2\left[\log R_{h_3 h} + G(M_{h_3}^2, M_Z^2) - G(M_h^2, M_Z^2)\right]\Bigg\}, \end{aligned} \tag{A.1}$$

$$\begin{aligned} T &= \frac{3}{16\pi \sin^2\theta_W}\Bigg\{\mathcal{R}_{11}^2\left[\frac{1}{\cos^2\theta_W}\left(\frac{\log R_{Zh_1}}{1-R_{Zh_1}} - \frac{\log R_{Zh}}{1-R_{Zh}}\right) - \left(\frac{\log R_{Wh_1}}{1-R_{Wh_1}} - \frac{\log R_{Wh}}{1-R_{Wh}}\right)\right] \\ &\quad + \mathcal{R}_{12}^2\left[\frac{1}{\cos^2\theta_W}\left(\frac{\log R_{Zh_2}}{1-R_{Zh_2}} - \frac{\log R_{Zh}}{1-R_{Zh}}\right) - \left(\frac{\log R_{Wh_2}}{1-R_{Wh_2}} - \frac{\log R_{Wh}}{1-R_{Wh}}\right)\right] \\ &\quad + \mathcal{R}_{13}^2\left[\frac{1}{\cos^2\theta_W}\left(\frac{\log R_{Zh_3}}{1-R_{Zh_3}} - \frac{\log R_{Zh}}{1-R_{Zh}}\right) - \left(\frac{\log R_{Wh_3}}{1-R_{Wh_3}} - \frac{\log R_{Wh}}{1-R_{Wh}}\right)\right]\Bigg\}, \end{aligned} \tag{A.2}$$

where the functions R_{AB}, $G(m_A^2, m_B^2)$, and $f(R_{AB})$ are given by

$$R_{AB} = \frac{M_A^2}{M_B^2}\,, \tag{A.3}$$

$$\begin{aligned} G(M_A^2, M_B^2) &= -\frac{79}{3} + 9R_{AB} - 2R_{AB}^2 + (12 - 4R_{AB} + R_{AB}^2) f(R_{AB}) \\ &\quad + (-10 + 18R_{AB} - 6R_{AB}^2 + R_{AB}^3 - 9\frac{R_{AB}+1}{R_{AB}-1}) \log R_{AB}, \end{aligned} \tag{A.4}$$

$$f(R_{AB}) = \begin{cases} \sqrt{R_{AB}(R_{AB}-4)} \log \left| \frac{R_{AB}-2-\sqrt{R_{AB}(R_{AB}-4)}}{2} \right| & R_{AB} > 4, \\ 0 & R_{AB} = 4, \\ 2\sqrt{R_{AB}(4-R_{AB})} \arctan \sqrt{\frac{4-R_{AB}}{R_{AB}}} & R_{AB} < 4. \end{cases} \tag{A.5}$$

B. RGEs

In this appendix, we present the two-loop gauge RGEs, as well as the one-loop RGEs for the Yukawa and scalar couplings. However, in our numerical analysis we used the full set of two-loop RGEs obtained using `SARAH` [165, 166]. Defining $\beta_\kappa \equiv (4\pi)^2 \frac{d\kappa}{d\ln\mu}$, the RGEs have the form

$$\beta_{g_1} = \frac{41}{10} g_1^3 + \frac{1}{(4\pi)^2} \frac{1}{50} g_1^3 \Big(199 g_1^2 + 135 g_2^2 + 440 g_3^2 - 85 y_t^2 \Big), \tag{B.1}$$

$$\beta_{g_2} = -\frac{19}{6} g_2^3 + \frac{1}{(4\pi)^2} \frac{1}{30} g_2^3 \Big(27 g_1^2 + 175 g_2^2 + 360 g_3^2 - 45 y_t^2 \Big), \tag{B.2}$$

$$\beta_{g_3} = -7 g_3^3 + \frac{1}{(4\pi)^2} \frac{1}{10} g_3^3 \Big(11 g_1^2 + 45 g_2^2 - 260 g_3^2 - 20 y_t^2 \Big), \tag{B.3}$$

$$\beta_{g_X} = -\frac{32}{3} g_X^3 - \frac{1}{(4\pi)^2} \frac{284}{3} g_X^5, \tag{B.4}$$

$$\beta_{y_t} = y_t \left(\frac{9}{2} y_t^2 - \frac{17}{20} g_1^2 - \frac{9}{4} g_2^2 - 8 g_3^2 \right), \tag{B.5}$$

$$\beta_{\lambda_h} = -6 y_t^4 + 24 \lambda_h^2 + \lambda_h \left(12 y_t^2 - \frac{9}{5} g_1^2 - 9 g_2^2 \right) + \frac{27}{200} g_1^4 + \frac{9}{20} g_1^2 g_2^2 + \frac{9}{8} g_2^4 + 3\lambda_{h1}^2 + 3\lambda_{h2}^2, \tag{B.6}$$

$$\beta_{\lambda_1} = -16 g_X^2 \lambda_1 + 28 \lambda_1^2 - 2\lambda_3 \lambda_4 + 2\lambda_{h1}^2 + 3\lambda_3^2 + \frac{13}{6} g_X^4 + \lambda_4^2 + \lambda_5^2, \tag{B.7}$$

$$\beta_{\lambda_2} = -16 g_X^2 \lambda_2 + 28 \lambda_2^2 - 2\lambda_3 \lambda_4 + 2\lambda_{h2}^2 + 3\lambda_3^2 + \frac{13}{6} g_X^4 + \lambda_4^2 + \lambda_5^2, \tag{B.8}$$

$$\beta_{\lambda_{h1}} = \lambda_{h1} \left(-\frac{9}{10} g_1^2 - \frac{9}{2} g_2^2 - 8 g_X^2 + 12 \lambda_h - 4\lambda_{h1} + 16 \lambda_1 + 6 y_t^2 \right) + 6\lambda_{h2}\lambda_3 - 2\lambda_{h2}\lambda_4, \tag{B.9}$$

$$\beta_{\lambda_{h2}} = \lambda_{h2}\left(-\frac{9}{10}g_1^2 - \frac{9}{2}g_2^2 - 8g_X^2 + 12\lambda_h - 4\lambda_{h2} + 16\lambda_1 + 6y_t^2\right) + 6\lambda_{h1}\lambda_3 - 2\lambda_{h1}\lambda_4, \tag{B.10}$$

$$\beta_{\lambda_3} = \lambda_3\left(-16g_X^2 + 16\lambda_2 + 16\lambda_1 - 4\lambda_3\right) - 2\lambda_4^2 - 2\lambda_5^2 - 4\lambda_1\lambda_4 - 4\lambda_2\lambda_4 + 4\lambda_{h1}\lambda_{h2} - \frac{11}{6}g_X^4, \tag{B.11}$$

$$\beta_{\lambda_4} = 10\lambda_5^2 - 16g_X^2\lambda_4 + 4\lambda_1\lambda_4 + 4\lambda_2\lambda_4 + 6\lambda_4^2 - 8\lambda_3\lambda_4 + \frac{5}{2}g_X^4, \tag{B.12}$$

$$\beta_{\lambda_5} = 4\lambda_5\left(-2\lambda_3 - 4g_X^2 + 4\lambda_4 + \lambda_1 + \lambda_2\right). \tag{B.13}$$

For the SM gauge couplings and the top quark Yukawa coupling we specify the boundary conditions at the top quark pole mass M_t [14, 86],

$$g_1(\mu = M_t) = \sqrt{\frac{5}{3}}\left(0.35830 + 0.00011\left(\frac{M_t}{\text{GeV}} - 173.34\right) - 0.00020\left(\frac{M_W - 80.384\text{ GeV}}{0.014\text{ GeV}}\right)\right), \tag{B.14}$$

$$g_2(\mu = M_t) = 0.64779 + 0.00004\left(\frac{M_t}{\text{GeV}} - 173.34\right) + 0.00011\left(\frac{M_W - 80.384\text{ GeV}}{0.014\text{ GeV}}\right), \tag{B.15}$$

$$g_3(\mu = M_t) = 1.1666 + 0.00314\left(\frac{\alpha_s(M_Z) - 0.1184}{0.0007}\right) - 0.00046\left(\frac{M_t}{\text{GeV}} - 173.34\right), \tag{B.16}$$

$$y_t(\mu = M_t) = 0.93690 + 0.00556\left(\frac{M_t}{\text{GeV}} - 173.34\right) - 0.00042\left(\frac{\alpha_s(M_Z) - 0.1184}{0.0007}\right), \tag{B.17}$$

whereas the dark gauge coupling is defined at the scale of the lightest dark gauge boson $g_X(M_{X^{3\prime}})$. The boundary conditions for the scalar couplings are specified at the renormalization scale Λ where the tree-level potential is minimized.

C. Kinematics

The expressions for the Mandelstam variables s, t, u in the center of mass (CM) frame for the general process $a + b \to c + d$ are

$$s = (E_a + E_b)^2, \tag{C.1}$$

$$t = m_a^2 + m_c^2 - 2E_aE_c + 2p_a(s)p_c(s)\cos\theta, \tag{C.2}$$

$$u = m_a^2 + m_d^2 - 2E_aE_d - 2p_a(s)p_d(s)\cos\theta, \tag{C.3}$$

where θ is the CM scattering angle and $p_i(s) = |\vec{p}_i|$. The energies E_a, E_b, E_c, E_d and the 3-momenta p_a, p_b, p_c, p_d can be expressed in terms of the CM energy squared s as

$$\begin{aligned} E_a &= \tfrac{1}{2\sqrt{s}}\left(s + m_a^2 - m_b^2\right), \quad E_b = \tfrac{1}{2\sqrt{s}}\left(s + m_b^2 - m_a^2\right), \\ E_c &= \tfrac{1}{2\sqrt{s}}\left(s + m_c^2 - m_d^2\right), \quad E_d = \tfrac{1}{2\sqrt{s}}\left(s + m_d^2 - m_c^2\right), \end{aligned} \tag{C.4}$$

$$\begin{aligned} p_{\rm in}(s) \equiv p_a(s) = p_b(s) &= \left[\tfrac{s}{4} - \tfrac{1}{2}(m_a^2 + m_b^2) + \tfrac{1}{4s}(m_a^2 - m_b^2)^2\right]^{1/2}, \\ p_{\rm out}(s) \equiv p_c(s) = p_d(s) &= \left[\tfrac{s}{4} - \tfrac{1}{2}(m_c^2 + m_d^2) + \tfrac{1}{4s}(m_c^2 - m_d^2)^2\right]^{1/2}. \end{aligned} \tag{C.5}$$

Using $s + t + u = m_a^2 + m_b^2 + m_c^2 + m_d^2$ we can write

$$t = \frac{1}{2}\left[m_a^2 + m_b^2 + m_c^2 + m_d^2 - s + (t-u)\right], \tag{C.6}$$

$$u = \frac{1}{2}\left[m_a^2 + m_b^2 + m_c^2 + m_d^2 - s - (t-u)\right], \tag{C.7}$$

and express $t - u$ as

$$t - u = -\frac{1}{s}(m_a^2 - m_b^2)(m_c^2 - m_d^2) + 4p_a(s)p_c(s)\cos\theta. \tag{C.8}$$

In view of the above, any function $f(s,t,u)$ is a function of s and the incoming momentum projection $p_{\rm in}(s)\cos\theta$. Finally, the relative velocity is

$$v_r = |\vec{\beta}_a - \vec{\beta}_b| = \frac{p_{\rm in}\sqrt{s}}{E_a E_b}. \tag{C.9}$$

References

[1] **ATLAS** Collaboration, G. Aad *et al.*, "Observation of a new particle in the search for the Standard Model Higgs boson with the ATLAS detector at the LHC," *Phys.Lett.* **B716** (2012) 1–29, arXiv:1207.7214 [hep-ex].

[2] **CMS** Collaboration, S. Chatrchyan *et al.*, "Observation of a new boson at a mass of 125 GeV with the CMS experiment at the LHC," *Phys.Lett.* **B716** (2012) 30–61, arXiv:1207.7235 [hep-ex].

[3] F. Englert and R. Brout, "Broken Symmetry and the Mass of Gauge Vector Mesons," *Phys.Rev.Lett.* **13** (1964) 321–323.

[4] P. W. Higgs, "Broken symmetries, massless particles and gauge fields," *Phys.Lett.* **12** (1964) 132–133.

[5] P. W. Higgs, "Broken Symmetries and the Masses of Gauge Bosons," *Phys.Rev.Lett.* **13** (1964) 508–509.

[6] G. Guralnik, C. Hagen, and T. Kibble, "Global Conservation Laws and Massless Particles," *Phys.Rev.Lett.* **13** (1964) 585–587.

[7] W. A. Bardeen, "On naturalness in the standard model,".

[8] S. R. Coleman and E. J. Weinberg, "Radiative Corrections as the Origin of Spontaneous Symmetry Breaking," *Phys.Rev.* **D7** (1973) 1888–1910.

[9] E. Gildener and S. Weinberg, "Symmetry Breaking and Scalar Bosons," *Phys.Rev.* **D13** (1976) 3333.

[10] **ATLAS, CMS** Collaboration, G. Aad *et al.*, "Combined Measurement of the Higgs Boson Mass in pp Collisions at $\sqrt{s} = 7$ and 8 TeV with the ATLAS and CMS Experiments," *Phys.Rev.Lett.* **114** (2015) 191803, arXiv:1503.07589 [hep-ex].

[11] A. Sirlin and R. Zucchini, "Dependence of the Quartic Coupling H(m) on M(H) and the Possible Onset of New Physics in the Higgs Sector of the Standard Model," *Nucl.Phys.* **B266** (1986) 389.

[12] M. Holthausen, K. S. Lim, and M. Lindner, "Planck scale Boundary Conditions and the Higgs Mass," *JHEP* **1202** (2012) 037, arXiv:1112.2415 [hep-ph].

[13] G. Degrassi, S. Di Vita, J. Elias-Miro, J. R. Espinosa, G. F. Giudice, *et al.*, "Higgs mass and vacuum stability in the Standard Model at NNLO," *JHEP* **1208** (2012) 098, arXiv:1205.6497 [hep-ph].

[14] D. Buttazzo, G. Degrassi, P. P. Giardino, G. F. Giudice, F. Sala, *et al.*, "Investigating the near-criticality of the Higgs boson," *JHEP* **1312** (2013) 089, arXiv:1307.3536 [hep-ph].

[15] M. F. Zoller, "Vacuum stability in the SM and the three-loop β-function for the Higgs self-interaction," *Subnucl. Ser.* **50** (2014) 557–566, arXiv:1209.5609 [hep-ph].

[16] V. Branchina and E. Messina, "Stability, Higgs Boson Mass and New Physics," *Phys. Rev. Lett.* **111** (2013) 241801, arXiv:1307.5193 [hep-ph].

[17] V. Branchina, E. Messina, and A. Platania, "Top mass determination, Higgs inflation, and vacuum stability," *JHEP* **09** (2014) 182, arXiv:1407.4112 [hep-ph].

[18] A. Andreassen, W. Frost, and M. D. Schwartz, "Consistent Use of the Standard Model Effective Potential," *Phys.Rev.Lett.* **113** no. 24, (2014) 241801, arXiv:1408.0292 [hep-ph].

[19] V. Branchina, E. Messina, and M. Sher, "Lifetime of the electroweak vacuum and sensitivity to Planck scale physics," *Phys. Rev.* **D91** (2015) 013003, arXiv:1408.5302 [hep-ph].

[20] F. Bezrukov, J. Rubio, and M. Shaposhnikov, "Living beyond the edge: Higgs inflation and vacuum metastability," *Phys. Rev.* **D92** no. 8, (2015) 083512, arXiv:1412.3811 [hep-ph].

[21] J. R. Espinosa, G. F. Giudice, E. Morgante, A. Riotto, L. Senatore, A. Strumia, and N. Tetradis, "The cosmological Higgstory of the vacuum instability," *JHEP* **09** (2015) 174, arXiv:1505.04825 [hep-ph].

[22] A. V. Bednyakov, B. A. Kniehl, A. F. Pikelner, and O. L. Veretin, "Stability of the Electroweak Vacuum: Gauge Independence and Advanced Precision," *Phys. Rev. Lett.* **115** no. 20, (2015) 201802, arXiv:1507.08833 [hep-ph].

[23] A. G. Dias, "Neutrino Mass Through Concomitant Breakdown of the U(1) Chiral and Scale Symmetries," *Phys. Rev.* **D73** (2006) 096002, arXiv:hep-ph/0604219 [hep-ph].

[24] K. A. Meissner and H. Nicolai, "Conformal Symmetry and the Standard Model," *Phys.Lett.* **B648** (2007) 312–317, arXiv:hep-th/0612165 [hep-th].

[25] R. Foot, A. Kobakhidze, and R. R. Volkas, "Electroweak Higgs as a pseudo-Goldstone boson of broken scale invariance," *Phys.Lett.* **B655** (2007) 156–161, arXiv:0704.1165 [hep-ph].

[26] R. Foot, A. Kobakhidze, K. McDonald, and R. Volkas, "Neutrino mass in radiatively-broken scale-invariant models," *Phys.Rev.* **D76** (2007) 075014, arXiv:0706.1829 [hep-ph].

[27] R. Foot, A. Kobakhidze, K. L. McDonald, and R. R. Volkas, "A Solution to the hierarchy problem from an almost decoupled hidden sector within a classically scale invariant theory," *Phys.Rev.* **D77** (2008) 035006, arXiv:0709.2750 [hep-ph].

[28] R. Foot, A. Kobakhidze, and R. R. Volkas, "Stable mass hierarchies and dark matter from hidden sectors in the scale-invariant standard model," *Phys.Rev.* **D82** (2010) 035005, arXiv:1006.0131 [hep-ph].

[29] L. Alexander-Nunneley and A. Pilaftsis, "The Minimal Scale Invariant Extension of the Standard Model," *JHEP* **1009** (2010) 021, arXiv:1006.5916 [hep-ph].

[30] R. Foot, A. Kobakhidze, and R. R. Volkas, "Cosmological constant in scale-invariant theories," *Phys. Rev.* **D84** (2011) 075010, arXiv:1012.4848 [hep-ph].

[31] R. Foot and A. Kobakhidze, "Electroweak Scale Invariant Models with Small Cosmological Constant," arXiv:1112.0607 [hep-ph].

[32] K. Ishiwata, "Dark Matter in Classically Scale-Invariant Two Singlets Standard Model," *Phys.Lett.* **B710** (2012) 134–138, arXiv:1112.2696 [hep-ph].

[33] J. S. Lee and A. Pilaftsis, "Radiative Corrections to Scalar Masses and Mixing in a Scale Invariant Two Higgs Doublet Model," *Phys.Rev.* **D86** (2012) 035004, arXiv:1201.4891 [hep-ph].

[34] A. Farzinnia, H.-J. He, and J. Ren, "Natural Electroweak Symmetry Breaking from Scale Invariant Higgs Mechanism," *Phys. Lett.* **B727** (2013) 141–150, arXiv:1308.0295 [hep-ph].

[35] D. Chway, T. H. Jung, H. D. Kim, and R. Dermisek, "Radiative Electroweak Symmetry Breaking Model Perturbative All the Way to the Planck Scale," *Phys. Rev. Lett.* **113**

no. 5, (2014) 051801, arXiv:1308.0891 [hep-ph].

[36] M. Lindner, S. Schmidt, and J. Smirnov, "Neutrino Masses and Conformal Electro-Weak Symmetry Breaking," *JHEP* **1410** (2014) 177, arXiv:1405.6204 [hep-ph].

[37] H. Davoudiasl and I. M. Lewis, "Right-Handed Neutrinos as the Origin of the Electroweak Scale," *Phys.Rev.* **D90** no. 3, (2014) 033003, arXiv:1404.6260 [hep-ph].

[38] E. Gabrielli, M. Heikinheimo, K. Kannike, A. Racioppi, M. Raidal, *et al.*, "Towards Completing the Standard Model: Vacuum Stability, EWSB and Dark Matter," *Phys.Rev.* **D89** no. 1, (2014) 015017, arXiv:1309.6632 [hep-ph].

[39] O. Antipin, M. Mojaza, and F. Sannino, "Conformal Extensions of the Standard Model with Veltman Conditions," *Phys.Rev.* **D89** no. 8, (2014) 085015, arXiv:1310.0957 [hep-ph].

[40] J. Guo and Z. Kang, "Higgs Naturalness and Dark Matter Stability by Scale Invariance," *Nucl. Phys.* **B898** (2015) 415–430, arXiv:1401.5609 [hep-ph].

[41] A. Farzinnia and J. Ren, "Higgs Partner Searches and Dark Matter Phenomenology in a Classically Scale Invariant Higgs Boson Sector," *Phys.Rev.* **D90** no. 1, (2014) 015019, arXiv:1405.0498 [hep-ph].

[42] K. Kannike, A. Racioppi, and M. Raidal, "Embedding inflation into the Standard Model - more evidence for classical scale invariance," *JHEP* **1406** (2014) 154, arXiv:1405.3987 [hep-ph].

[43] Z. Kang, "Upgrading sterile neutrino dark matter to FImP using scale invariance," *Eur. Phys. J.* **C75** no. 10, (2015) 471, arXiv:1411.2773 [hep-ph].

[44] P. Humbert, M. Lindner, and J. Smirnov, "The Inverse Seesaw in Conformal Electro-Weak Symmetry Breaking and Phenomenological Consequences," arXiv:1503.03066 [hep-ph].

[45] K. Endo and Y. Sumino, "A Scale-invariant Higgs Sector and Structure of the Vacuum," *JHEP* **05** (2015) 030, arXiv:1503.02819 [hep-ph].

[46] F. Sannino and J. Virkajrvi, "First Order Electroweak Phase Transition from (Non)Conformal Extensions of the Standard Model," *Phys. Rev.* **D92** no. 4, (2015) 045015, arXiv:1505.05872 [hep-ph].

[47] Z. Kang, "View FImP miracle (by scale invariance) la self-interaction," *Phys. Lett.* **B751** (2015) 201–204, arXiv:1505.06554 [hep-ph].

[48] K. Endo and K. Ishiwata, "Direct detection of singlet dark matter in classically scale-invariant standard model," *Phys. Lett.* **B749** (2015) 583–588, arXiv:1507.01739 [hep-ph].

[49] A. Farzinnia, "Prospects for Discovering the Higgs-like Pseudo-Nambu-Goldstone Boson of the Classical Scale Symmetry," *Phys. Rev.* **D92** no. 9, (2015) 095012, arXiv:1507.06926 [hep-ph].

[50] K. Endo, K. Ishiwata, and Y. Sumino, "WW scattering in a radiative electroweak symmetry breaking scenario," arXiv:1601.00696 [hep-ph].

[51] A. Ahriche, K. L. McDonald, and S. Nasri, "A Radiative Model for the Weak Scale and Neutrino Mass via Dark Matter," *JHEP* **02** (2016) 038, arXiv:1508.02607 [hep-ph].

[52] Z.-W. Wang, T. G. Steele, T. Hanif, and R. B. Mann, "Conformal Complex Singlet Extension of the Standard Model: Scenario for Dark Matter and a Second Higgs Boson," arXiv:1510.04321 [hep-ph].

[53] K. Ghorbani and H. Ghorbani, "Scalar Dark Matter in Scale Invariant Standard Model," *JHEP* **04** (2016) 024, arXiv:1511.08432 [hep-ph].

[54] A. Farzinnia and S. Kouwn, "Classically scale invariant inflation, supermassive WIMPs, and adimensional gravity," *Phys. Rev.* **D93** no. 6, (2016) 063528, arXiv:1512.05890 [hep-ph].

[55] A. J. Helmboldt, P. Humbert, M. Lindner, and J. Smirnov, "Minimal Conformal Extensions of the Higgs Sector," arXiv:1603.03603 [hep-ph].

[56] P. G. Ferreira, C. T. Hill, and G. G. Ross, "Scale-Independent Inflation and Hierarchy Generation," *Submitted to: Phys. Rev. Lett.* (2016) , arXiv:1603.05983 [hep-th].

[57] A. Ahriche, K. L. McDonald, and S. Nasri, "The Scale-Invariant Scotogenic Model," arXiv:1604.05569 [hep-ph].

[58] A. Ahriche, A. Manning, K. L. McDonald, and S. Nasri, "Scale-Invariant Models with One-Loop Neutrino Mass and Dark Matter Candidates," arXiv:1604.05995 [hep-ph].

[59] K. Kawana, "Classical conformality in the Standard Model from Coleman's theory," arXiv:1605.00436 [hep-ph].

[60] F. Wu, "Aspects of a Non-minimal Conformal Extension of the Standard Model," arXiv:1606.08112 [hep-ph].

[61] L. Marzola and A. Racioppi, "Minimal but non-minimal inflation and electroweak symmetry breaking," arXiv:1606.06887 [hep-ph].

[62] R. Hempfling, "The Next-to-minimal Coleman-Weinberg model," *Phys.Lett.* **B379** (1996) 153–158, arXiv:hep-ph/9604278 [hep-ph].

[63] W.-F. Chang, J. N. Ng, and J. M. Wu, "Shadow Higgs from a scale-invariant hidden U(1)(s) model," *Phys.Rev.* **D75** (2007) 115016, arXiv:hep-ph/0701254 [HEP-PH].

[64] S. Iso, N. Okada, and Y. Orikasa, "Classically conformal B^- L extended Standard Model," *Phys.Lett.* **B676** (2009) 81–87, arXiv:0902.4050 [hep-ph].

[65] S. Iso, N. Okada, and Y. Orikasa, "The minimal B-L model naturally realized at TeV scale," *Phys.Rev.* **D80** (2009) 115007, arXiv:0909.0128 [hep-ph].

[66] M. Holthausen, M. Lindner, and M. A. Schmidt, "Radiative Symmetry Breaking of the Minimal Left-Right Symmetric Model," *Phys.Rev.* **D82** (2010) 055002, arXiv:0911.0710 [hep-ph].

[67] S. Iso and Y. Orikasa, "TeV Scale B-L model with a flat Higgs potential at the Planck scale - in view of the hierarchy problem -," *PTEP* **2013** (2013) 023B08, arXiv:1210.2848

[hep-ph].

[68] C. Englert, J. Jaeckel, V. Khoze, and M. Spannowsky, "Emergence of the Electroweak Scale through the Higgs Portal," *JHEP* **1304** (2013) 060, arXiv:1301.4224 [hep-ph].

[69] E. J. Chun, S. Jung, and H. M. Lee, "Radiative generation of the Higgs potential," *Phys. Lett.* **B725** (2013) 158–163, arXiv:1304.5815 [hep-ph]. [Erratum: Phys. Lett.B730,357(2014)].

[70] R. S. Chivukula, A. Farzinnia, J. Ren, and E. H. Simmons, "Constraints on the Scalar Sector of the Renormalizable Coloron Model," *Phys. Rev.* **D88** no. 7, (2013) 075020, arXiv:1307.1064 [hep-ph]. [Erratum: Phys. Rev.D89,no.5,059905(2014)].

[71] V. V. Khoze and G. Ro, "Leptogenesis and Neutrino Oscillations in the Classically Conformal Standard Model with the Higgs Portal," *JHEP* **1310** (2013) 075, arXiv:1307.3764.

[72] V. V. Khoze, "Inflation and Dark Matter in the Higgs Portal of Classically Scale Invariant Standard Model," *JHEP* **1311** (2013) 215, arXiv:1308.6338 [hep-ph].

[73] T. Hambye and A. Strumia, "Dynamical generation of the weak and Dark Matter scale," *Phys.Rev.* **D88** (2013) 055022, arXiv:1306.2329 [hep-ph].

[74] C. D. Carone and R. Ramos, "Classical scale-invariance, the electroweak scale and vector dark matter," *Phys.Rev.* **D88** (2013) 055020, arXiv:1307.8428 [hep-ph].

[75] M. Heikinheimo, A. Racioppi, M. Raidal, C. Spethmann, and K. Tuominen, "Physical Naturalness and Dynamical Breaking of Classical Scale Invariance," *Mod.Phys.Lett.* **A29** (2014) 1450077, arXiv:1304.7006 [hep-ph].

[76] M. Holthausen, J. Kubo, K. S. Lim, and M. Lindner, "Electroweak and Conformal Symmetry Breaking by a Strongly Coupled Hidden Sector," *JHEP* **1312** (2013) 076, arXiv:1310.4423 [hep-ph].

[77] M. Hashimoto, S. Iso, and Y. Orikasa, "Radiative symmetry breaking at the Fermi scale and flat potential at the Planck scale," *Phys.Rev.* **D89** no. 1, (2014) 016019, arXiv:1310.4304 [hep-ph].

[78] S. Benic and B. Radovcic, "Electroweak breaking and Dark Matter from the common scale," *Phys. Lett.* **B732** (2014) 91–94, arXiv:1401.8183 [hep-ph].

[79] V. V. Khoze, C. McCabe, and G. Ro, "Higgs vacuum stability from the dark matter portal," *JHEP* **08** (2014) 026, arXiv:1403.4953 [hep-ph].

[80] S. Benic and B. Radovcic, "Majorana dark matter in a classically scale invariant model," *JHEP* **01** (2015) 143, arXiv:1409.5776 [hep-ph].

[81] J. Kubo, K. S. Lim, and M. Lindner, "Gamma-ray Line from Nambu-Goldstone Dark Matter in a Scale Invariant Extension of the Standard Model," *JHEP* **09** (2014) 016, arXiv:1405.1052 [hep-ph].

[82] G. M. Pelaggi, "Predictions of a model of weak scale from dynamical breaking of scale invariance," *Nucl.Phys.* **B893** (2015) 443–458, arXiv:1406.4104 [hep-ph].

[83] J. Guo, Z. Kang, P. Ko, and Y. Orikasa, "Accidental dark matter: Case in the scale invariant local B-L model," *Phys. Rev.* **D91** no. 11, (2015) 115017, arXiv:1502.00508 [hep-ph].

[84] N. Haba, H. Ishida, N. Okada, and Y. Yamaguchi, "Bosonic seesaw mechanism in a classically conformal extension of the Standard Model," *Phys. Lett.* **B754** (2016) 349–352, arXiv:1508.06828 [hep-ph].

[85] Y. Orikasa, "The Classically Conformal B−L Extended Ma Model," arXiv:1504.07953 [hep-ph].

[86] S. Oda, N. Okada, and D.-s. Takahashi, "Classically conformal U(1) extended standard model and Higgs vacuum stability," *Phys. Rev.* **D92** no. 1, (2015) 015026, arXiv:1504.06291 [hep-ph].

[87] N. Haba and Y. Yamaguchi, "Vacuum stability in the $U(1)_\chi$ extended model with vanishing scalar potential at the Planck scale," *PTEP* **2015** no. 9, (2015) 093B05, arXiv:1504.05669 [hep-ph].

[88] Y. Ametani, M. Aoki, H. Goto, and J. Kubo, "Nambu-Goldstone Dark Matter in a Scale Invariant Bright Hidden Sector," *Phys. Rev.* **D91** no. 11, (2015) 115007, arXiv:1505.00128 [hep-ph].

[89] C. D. Carone and R. Ramos, "Dark chiral symmetry breaking and the origin of the electroweak scale," *Phys. Lett.* **B746** (2015) 424–429, arXiv:1505.04448 [hep-ph].

[90] W. Altmannshofer, W. A. Bardeen, M. Bauer, M. Carena, and J. D. Lykken, "Light Dark Matter, Naturalness, and the Radiative Origin of the Electroweak Scale," *JHEP* **1501** (2015) 032, arXiv:1408.3429 [hep-ph].

[91] A. D. Plascencia, "Classical scale invariance in the inert doublet model," *JHEP* **09** (2015) 026, arXiv:1507.04996 [hep-ph].

[92] A. Karam and K. Tamvakis, "Dark matter and neutrino masses from a scale-invariant multi-Higgs portal," *Phys. Rev.* **D92** no. 7, (2015) 075010, arXiv:1508.03031 [hep-ph].

[93] Z.-W. Wang, F. S. Sage, T. G. Steele, and R. B. Mann, "Can an Asymptotically-Safe Conformal $U(1)'$ Model Address the LHC Diboson Excess?," arXiv:1511.02531 [hep-ph].

[94] A. Das, N. Okada, and N. Papapietro, "Electroweak vacuum stability in classically conformal B-L extension of the Standard Model," arXiv:1509.01466 [hep-ph].

[95] N. Haba, H. Ishida, R. Takahashi, and Y. Yamaguchi, "Gauge coupling unification in a classically scale invariant model," *JHEP* **02** (2016) 058, arXiv:1511.02107 [hep-ph].

[96] H. Okada, Y. Orikasa, and K. Yagyu, "Higgs Triplet Model with Classically Conformal Invariance," arXiv:1510.00799 [hep-ph].

[97] A. Karam and K. Tamvakis, "Dark matter and neutrino masses from a classically scale-invariant multi-Higgs portal," in *15th Hellenic School and Workshops on Elementary Particle Physics and Gravity (CORFU2015) Corfu, Greece, September 1-26, 2015*. 2016.

arXiv:1603.08470 [hep-ph].

[98] R. Jinno and M. Takimoto, "Probing classically conformal $B - L$ model with gravitational waves," arXiv:1604.05035 [hep-ph].

[99] A. Das, S. Oda, N. Okada, and D.-s. Takahashi, "Classically conformal U(1)' extended standard model, electroweak vacuum stability, and LHC Run-2 bounds," *Phys. Rev.* **D93** no. 11, (2016) 115038, arXiv:1605.01157 [hep-ph].

[100] V. V. Khoze and A. D. Plascencia, "Dark Matter and Leptogenesis Linked by Classical Scale Invariance," arXiv:1605.06834 [hep-ph].

[101] K. Kannike, G. M. Pelaggi, A. Salvio, and A. Strumia, "The diphoton as the Higgs of the Higgs," arXiv:1605.08681 [hep-ph].

[102] H. Hatanaka, D.-W. Jung, and P. Ko, "AdS/QCD approach to the scale invariant extension of the standard model with a strongly interacting hidden sector," arXiv:1606.02969 [hep-ph].

[103] C. Gross, O. Lebedev, and Y. Mambrini, "Non-Abelian gauge fields as dark matter," *JHEP* **08** (2015) 158, arXiv:1505.07480 [hep-ph].

[104] K. Kannike, "Vacuum Stability Conditions From Copositivity Criteria," *Eur.Phys.J.* **C72** (2012) 2093, arXiv:1205.3781 [hep-ph].

[105] J. Chakrabortty, P. Konar, and T. Mondal, "Copositive Criteria and Boundedness of the Scalar Potential," *Phys. Rev.* **D89** no. 9, (2014) 095008, arXiv:1311.5666 [hep-ph].

[106] K. Kannike, "Vacuum stability of a general scalar potential of a few fields," *Eur.Phys.J. C* **76** (Mar., 2016) 324, 1603.02680.

[107] K. Cheung, J. S. Lee, and P.-Y. Tseng, "Higgs precision analysis updates 2014," *Phys. Rev.* **D90** (2014) 095009, arXiv:1407.8236 [hep-ph].

[108] **ATLAS** Collaboration, G. Aad *et al.*, "Measurements of Higgs boson production and couplings in the four-lepton channel in pp collisions at center-of-mass energies of 7 and 8 TeV with the ATLAS detector," *Phys. Rev.* **D91** no. 1, (2015) 012006, arXiv:1408.5191 [hep-ex].

[109] **CMS** Collaboration, V. Khachatryan *et al.*, "Precise determination of the mass of the Higgs boson and tests of compatibility of its couplings with the standard model predictions using proton collisions at 7 and 8 TeV," *Eur. Phys. J.* **C75** no. 5, (2015) 212, arXiv:1412.8662 [hep-ex].

[110] A. Falkowski, C. Gross, and O. Lebedev, "A second Higgs from the Higgs portal," *JHEP* **1505** (2015) 057, arXiv:1502.01361 [hep-ph].

[111] **Particle Data Group** Collaboration, K. A. Olive *et al.*, "Review of Particle Physics," *Chin. Phys.* **C38** (2014) 090001.

[112] **Planck** Collaboration, P. A. R. Ade *et al.*, "Planck 2015 results. XIII. Cosmological parameters," arXiv:1502.01589 [astro-ph.CO].

[113] T. Hambye, "Hidden vector dark matter," *JHEP* **0901** (2009) 028, arXiv:0811.0172 [hep-ph].

[114] T. Hambye and M. H. Tytgat, "Confined hidden vector dark matter," *Phys.Lett.* **B683** (2010) 39–41, arXiv:0907.1007 [hep-ph].

[115] H. Zhang, C. S. Li, Q.-H. Cao, and Z. Li, "A Dark Matter Model with Non-Abelian Gauge Symmetry," *Phys.Rev.* **D82** (2010) 075003, arXiv:0910.2831 [hep-ph].

[116] C. Arina, T. Hambye, A. Ibarra, and C. Weniger, "Intense Gamma-Ray Lines from Hidden Vector Dark Matter Decay," *JCAP* **1003** (2010) 024, arXiv:0912.4496 [hep-ph].

[117] S. Bhattacharya, J. L. Diaz-Cruz, E. Ma, and D. Wegman, "Dark Vector-Gauge-Boson Model," *Phys.Rev.* **D85** (2012) 055008, arXiv:1107.2093 [hep-ph].

[118] C.-W. Chiang, T. Nomura, and J. Tandean, "Nonabelian Dark Matter with Resonant Annihilation," *JHEP* **1401** (2014) 183, arXiv:1306.0882 [hep-ph].

[119] C. Boehm, M. J. Dolan, and C. McCabe, "A weighty interpretation of the Galactic Centre excess," *Phys.Rev.* **D90** no. 2, (2014) 023531, arXiv:1404.4977 [hep-ph].

[120] S. Baek, P. Ko, W.-I. Park, and E. Senaha, "Higgs Portal Vector Dark Matter : Revisited," *JHEP* **05** (2013) 036, arXiv:1212.2131 [hep-ph].

[121] F. D'Eramo, M. McCullough, and J. Thaler, "Multiple Gamma Lines from Semi-Annihilation," *JCAP* **1304** (2013) 030, arXiv:1210.7817 [hep-ph].

[122] Y. Farzan and A. R. Akbarieh, "VDM: A model for Vector Dark Matter," *JCAP* **1210** (2012) 026, arXiv:1207.4272 [hep-ph].

[123] A. Djouadi, O. Lebedev, Y. Mambrini, and J. Quevillon, "Implications of LHC searches for Higgs–portal dark matter," *Phys. Lett.* **B709** (2012) 65–69, arXiv:1112.3299 [hep-ph].

[124] K.-Y. Choi, H. M. Lee, and O. Seto, "Vector Higgs-portal dark matter and Fermi-LAT gamma ray line," *Phys. Rev.* **D87** no. 12, (2013) 123541, arXiv:1304.0966 [hep-ph].

[125] S. Baek, P. Ko, and W.-I. Park, "Hidden sector monopole, vector dark matter and dark radiation with Higgs portal," *JCAP* **1410** no. 10, (2014) 067, arXiv:1311.1035 [hep-ph].

[126] S. Baek, P. Ko, W.-I. Park, and Y. Tang, "Indirect and direct signatures of Higgs portal decaying vector dark matter for positron excess in cosmic rays," *JCAP* **1406** (2014) 046, arXiv:1402.2115 [hep-ph].

[127] P. Ko, W.-I. Park, and Y. Tang, "Higgs portal vector dark matter for GeV scale γ-ray excess from galactic center," *JCAP* **1409** (2014) 013, arXiv:1404.5257 [hep-ph].

[128] C. Balzs and T. Li, "Simplified Dark Matter Models Confront the Gamma Ray Excess," *Phys. Rev.* **D90** no. 5, (2014) 055026, arXiv:1407.0174 [hep-ph].

[129] Y. Farzan and A. R. Akbarieh, "Decaying Vector Dark Matter as an Explanation for the 3.5 keV Line from Galaxy Clusters," *JCAP* **1411** no. 11, (2014) 015, arXiv:1408.2950 [hep-ph].

[130] S. Fraser, E. Ma, and M. Zakeri, "$SU(2)_N$ model of vector dark matter with a leptonic

connection," *Int. J. Mod. Phys.* **A30** no. 03, (2015) 1550018, arXiv:1409.1162 [hep-ph].

[131] C.-R. Chen, Y.-K. Chu, and H.-C. Tsai, "An Elusive Vector Dark Matter," *Phys. Lett.* **B741** (2015) 205–209, arXiv:1410.0918 [hep-ph].

[132] W. Chao, "First order electroweak phase transition triggered by the Higgs portal vector dark matter," *Phys. Rev.* **D92** no. 1, (2015) 015025, arXiv:1412.3823 [hep-ph].

[133] M. Duch, B. Grzadkowski, and M. McGarrie, "A stable Higgs portal with vector dark matter," *JHEP* **09** (2015) 162, arXiv:1506.08805 [hep-ph].

[134] S. Di Chiara and K. Tuominen, "A minimal model for SU(N) vector dark matter," *JHEP* **11** (2015) 188, arXiv:1506.03285 [hep-ph].

[135] N. Bernal, X. Chu, C. Garcia-Cely, T. Hambye, and B. Zaldivar, "Production Regimes for Self-Interacting Dark Matter," *JCAP* **1603** no. 03, (2016) 018, arXiv:1510.08063 [hep-ph].

[136] F. S. Sage and R. Dick, "Gamma ray signals of the annihilation of Higgs-portal singlet dark matter," arXiv:1604.04589 [astro-ph.HE].

[137] V. V. Khoze and G. Ro, "Dark matter monopoles, vectors and photons," *JHEP* **10** (2014) 61, arXiv:1406.2291 [hep-ph].

[138] L. Bian, T. Li, J. Shu, and X.-C. Wang, "Two component dark matter with multi-Higgs portals," *JHEP* **1503** (2015) 126, arXiv:1412.5443 [hep-ph].

[139] C.-H. Chen and T. Nomura, "$SU(2)_X$ vector DM and Galactic Center gamma-ray excess," *Phys.Lett.* **B746** (2015) 351–358, arXiv:1501.07413 [hep-ph].

[140] C.-H. Chen, C.-W. Chiang, and T. Nomura, "Dark matter for excess of AMS-02 positrons and antiprotons," *Phys. Lett.* **B747** (2015) 495–499, arXiv:1504.07848 [hep-ph].

[141] C.-H. Chen and T. Nomura, "Searching for Vector Dark Matter by Higgs Portal at the LHC," arXiv:1507.00886 [hep-ph].

[142] V. V. Khoze, C. McCabe, and G. Ro, "Higgs vacuum stability from the dark matter portal," *JHEP* **1408** (2014) 026, arXiv:1403.4953 [hep-ph].

[143] A. DiFranzo, P. J. Fox, and T. M. P. Tait, "Vector Dark Matter through a Radiative Higgs Portal," *JHEP* **04** (2016) 135, arXiv:1512.06853 [hep-ph].

[144] P. Ko and H. Yokoya, "Search for Higgs portal DM at the ILC," arXiv:1603.04737 [hep-ph].

[145] J. Ellis, J. L. Evans, F. Luo, and K. A. Olive, "Scenarios for Gluino Coannihilation," *JHEP* **02** (2016) 071, arXiv:1510.03498 [hep-ph].

[146] F. D'Eramo and J. Thaler, "Semi-annihilation of Dark Matter," *JHEP* **1006** (2010) 109, arXiv:1003.5912 [hep-ph].

[147] P. Gondolo and G. Gelmini, "Cosmic abundances of stable particles: Improved analysis," *Nucl. Phys.* **B360** (1991) 145–179.

[148] J. Edsjo and P. Gondolo, "Neutralino relic density including coannihilations," *Phys.Rev.*

D56 (1997) 1879–1894, arXiv:hep-ph/9704361 [hep-ph].

[149] J. R. Ellis, T. Falk, K. A. Olive, and M. Srednicki, "Calculations of neutralino-stau coannihilation channels and the cosmologically relevant region of MSSM parameter space," *Astropart. Phys.* **13** (2000) 181–213, arXiv:hep-ph/9905481 [hep-ph]. [Erratum: Astropart. Phys.15,413(2001)].

[150] T. Hahn, "Generating Feynman diagrams and amplitudes with FeynArts 3," *Comput. Phys. Commun.* **140** (2001) 418–431, arXiv:hep-ph/0012260 [hep-ph].

[151] T. Hahn and M. Perez-Victoria, "Automatized one loop calculations in four-dimensions and D-dimensions," *Comput. Phys. Commun.* **118** (1999) 153–165, arXiv:hep-ph/9807565 [hep-ph].

[152] S. Di Chiara, V. Keus, and O. Lebedev, "Stabilizing the Higgs potential with a Z′," *Phys.Lett.* **B744** (2015) 59–66, arXiv:1412.7036 [hep-ph].

[153] J. M. Cline, K. Kainulainen, P. Scott, and C. Weniger, "Update on scalar singlet dark matter," *Phys. Rev.* **D88** (2013) 055025, arXiv:1306.4710 [hep-ph].

[154] J. M. Alarcon, J. Martin Camalich, and J. A. Oller, "The chiral representation of the πN scattering amplitude and the pion-nucleon sigma term," *Phys. Rev.* **D85** (2012) 051503, arXiv:1110.3797 [hep-ph].

[155] P. Junnarkar and A. Walker-Loud, "Scalar strange content of the nucleon from lattice QCD," *Phys. Rev.* **D87** (2013) 114510, arXiv:1301.1114 [hep-lat].

[156] J. M. Alarcon, L. S. Geng, J. Martin Camalich, and J. A. Oller, "The strangeness content of the nucleon from effective field theory and phenomenology," *Phys. Lett.* **B730** (2014) 342–346, arXiv:1209.2870 [hep-ph].

[157] A. Crivellin, M. Hoferichter, and M. Procura, "Accurate evaluation of hadronic uncertainties in spin-independent WIMP-nucleon scattering: Disentangling two- and three-flavor effects," *Phys. Rev.* **D89** (2014) 054021, arXiv:1312.4951 [hep-ph].

[158] M. Hoferichter, J. Ruiz de Elvira, B. Kubis, and U.-G. Meiner, "High-Precision Determination of the Pion-Nucleon Term from Roy-Steiner Equations," *Phys. Rev. Lett.* **115** (2015) 092301, arXiv:1506.04142 [hep-ph].

[159] M. Aoki, M. Duerr, J. Kubo, and H. Takano, "Multi-Component Dark Matter Systems and Their Observation Prospects," *Phys. Rev.* **D86** (2012) 076015, arXiv:1207.3318 [hep-ph].

[160] M. Aoki, J. Kubo, and H. Takano, "Multicomponent Dark Matter in Radiative Seesaw Model and Monochromatic Neutrino Flux," *Phys.Rev.* **D90** no. 7, (2014) 076011, arXiv:1408.1853 [hep-ph].

[161] S. Esch, M. Klasen, and C. E. Yaguna, "A minimal model for two-component dark matter," *JHEP* **09** (2014) 108, arXiv:1406.0617 [hep-ph].

[162] **LUX** Collaboration, D. S. Akerib *et al.*, "First results from the LUX dark matter experiment at the Sanford Underground Research Facility," *Phys. Rev. Lett.* **112** (2014)

091303, arXiv:1310.8214 [astro-ph.CO].

[163] D. C. Malling *et al.*, "After LUX: The LZ Program," arXiv:1110.0103 [astro-ph.IM].

[164] **XENON** Collaboration, E. Aprile *et al.*, "Physics reach of the XENON1T dark matter experiment," *JCAP* **1604** no. 04, (2016) 027, arXiv:1512.07501 [physics.ins-det].

[165] F. Staub, "SARAH 4 : A tool for (not only SUSY) model builders," *Comput. Phys. Commun.* **185** (2014) 1773–1790, arXiv:1309.7223 [hep-ph].

[166] F. Staub, "Exploring new models in all detail with SARAH," *Adv. High Energy Phys.* **2015** (2015) 840780, arXiv:1503.04200 [hep-ph].